(4)

NSWC MP 88-178

INVESTIGATION OF THE ORIGIN OF HOT SPOTS IN DEFORMED CRYSTALS: STUDIES ON AMMONIUM PERCHLORATE AND REFERENCE INERT MATERIALS

ANNUAL PROGRESS REPORT NO.1 FOR PERIOD 1 APRIL 1987 TO 31 MARCH 1988
UNDER WORK REQUEST NUMBER N00014-87-K-0175 (WORK UNIT NUMBER
432h-803) AND FOR PERIOD 1 OCTOBER 1986 TO 31 MARCH 1988
UNDER WORK REQUEST NUMBER N00014-85-WR-24103 (WORK UNIT NUMBER 432h-797)

W.L. ELBAN AND P.J. COYNE, JR.
DEPARTMENT OF ENGINEERING SCIENCE
LOYOLA COLLEGE
BALTIMORE, MD 21210

AND

H.W. SANDUSKY, B.C. GLANCY, AND D.W. CARLSON
RESEARCH AND TECHNOLOGY DEPARTMENT

AND

R.W. ARMSTRONG
MECHANICAL ENGINEERING DEPARTMENT
UNIVERSITY OF MARYLAND, COLLEGE PARK, MD 20742

APRIL 1988

PREPARED FOR
OFFICE OF NAVAL RESEARCH
800 N QUINCY STREET
ARLINGTON, VA 22217

NAVAL SURFACE WARFARE CENTER

Dahlgren, Virginia 22448-5000 • Silver Spring, Maryland 20903-5000

UNCLASSIFIED
SECURITY CLASSIFICATION OF THIS PAGE

REPORT DOCUMENTATION PAGE

1a. REPORT SECURITY CLASSIFICATION UNCLASSIFIED	1b. RESTRICTIVE MARKINGS
2a. SECURITY CLASSIFICATION AUTHORITY 2b. DECLASSIFICATION / DOWNGRADING SCHEDULE	3. DISTRIBUTION / AVAILABILITY OF REPORT Approved for public release; distribution is unlimited
4. PERFORMING ORGANIZATION REPORT NUMBER(S) NSWC MP 88-178	5. MONITORING ORGANIZATION REPORT NUMBER(S)
6a. NAME OF PERFORMING ORGANIZATION Naval Surface Warfare Center 6b. OFFICE SYMBOL (If applicable) R13	7a. NAME OF MONITORING ORGANIZATION
6c. ADDRESS (City, State, and ZIP Code) 10901 New Hampshire Avenue Silver Spring, MD 20903-5000	7b. ADDRESS (City, State, and ZIP Code)
8a. NAME OF FUNDING / SPONSORING ORGANIZATION Office of Naval Research 8b. OFFICE SYMBOL (If applicable) 1132P	9. PROCUREMENT INSTRUMENT IDENTIFICATION NUMBER
8c. ADDRESS (City, State, and ZIP Code) 800 N. Quincy Street Arlington, VA 22217	10. SOURCE OF FUNDING NUMBERS PROGRAM ELEMENT NO. 61153N PROJECT NO. RR024-02-0A TASK NO. 0 WORK UNIT ACCESSION NO. 432h-803 432h-797

11. TITLE (Include Security Classification)
Investigation of the Origin of Hot Spots in Deformed Crystals: Studies on Ammonium Perchlorate and Reference Inert Materials

12. PERSONAL AUTHOR(S) Elban, W. L., Coyne, Jr., P. J., Sandusky, H. W., Glancy, B. C., Carlson, D. W., Armstrong, R. W.

13a. TYPE OF REPORT	13b. TIME COVERED	14. DATE OF REPORT (Year, Month, Day)	15. PAGE COUNT
Progress	FROM 1/86 TO 3/88	1988 April	66

16. SUPPLEMENTARY NOTATION

17. COSATI CODES			18. SUBJECT TERMS (Continue on reverse if necessary and identify by block number)
FIELD	GROUP	SUB-GROUP	Ammonium Perchlorate; Polarized Light Microscopy; Hot Spot; Shock Reactivity; Microhardness; Liquid Ion Chromatography.
07	02		
20	11		

19. ABSTRACT (Continue on reverse if necessary and identify by block number)

Work is in progress to investigate the roles that mechanical deformation and resultant material microstructure have on the shock reactivity of ammonium perchlorate (AP) single crystals. The deformation and fracture behaviors of AP have been studied using microindentation hardness testing. The operative slip systems and cracking planes involved in forming diamond pyramid (Vickers) impressions were identified. Using polarized light microscopy, it was determined that the strain field caused by edge dislocations surrounding the hardness impression was rather far reaching. Single crystals placed in a mineral oil bath were shocked by exploding a detonator. High-speed photography was used to observe the crystal response to the shock wave, and samples were recovered for quantitative chemical analysis of decomposition products.

20. DISTRIBUTION / AVAILABILITY OF ABSTRACT ☐ UNCLASSIFIED/UNLIMITED ☒ SAME AS RPT. ☐ DTIC USERS	21. ABSTRACT SECURITY CLASSIFICATION Unclassified
22a. NAME OF RESPONSIBLE INDIVIDUAL H. W. Sandusky	22b. TELEPHONE (Include Area Code) (202) 394-1612 22c. OFFICE SYMBOL R13

DD FORM 1473, 84 MAR 83 APR edition may be used until exhausted. All other editions are obsolete

UNCLASSIFIED

U.S. Government Printing Office 1985—630-012

0102-LF-014-6602

FOREWORD

This work is being performed to determine the role that material microstructure has on the chemical reactivity of ammonium perchlorate (AP) single crystals subjected to weak shocks. Of particular interest is understanding how energy is locally concentrated in AP to form hot spots. Results and conclusions are presented concerning the deformation and fracture behaviors of AP determined from diamond pyramid (Vickers) hardness tests. Microsecond observations of structural changes during dynamic compression of AP crystals and measurements obtained of chemical decomposition products in recovered shocked crystals are also described.

This investigation was sponsored by the Office of Naval Research under work request numbers N00014-87-K-0175 and N00014-85-WR-24103 as a cooperative effort between Loyola College, Baltimore, and the Naval Surface Warfare Center, White Oak, including collaboration with the University of Maryland, College Park. The identification of manufacturers and/or products in this report does not imply endorsement or criticism by the Naval Surface Warfare Center.

Dr. Richard R. Bernecker provided many helpful comments and guidance concerning the direction of the research. Dr. Sigmund J. Jacobs made numerous helpful suggestions for improving this report. Dr. Donald A. Keefer, Department of Biology, Loyola College, helped with the microscopy used to obtain all of the photographs shown in this report. The work of Dr. Xian Jie Zhang, Department of Mechanical Engineering, University of Maryland, College Park, in printing the photographs appearing in Figures 8, 9, and 10 is gratefully acknowledged.

Approved by:

William H. Bohl for

KURT F. MUELLER, Head
Energetic Materials Division

CONTENTS

ILLUSTRATIONS

ILLUSTRATIONS (Cont.)

TABLES

INTRODUCTION

For initiation of chemical reaction to occur in crystalline explosives or oxidizers experiencing pressure-time histories typical of drop-weight impact conditions, the energy transferred must be localized within the material. A number of years ago Bowden and Yoffe[1] at the Cavendish Laboratory, Cambridge University, proposed and experimentally demonstrated the existence of localized regions in crystalline energetic materials (explosives or oxidizers) that were undergoing preferential chemical decomposition as a result of the materials experiencing mechanical forces. In response to the mechanical forces, heat is generated within small volumes of the material at a sufficient rate to cause chemical decomposition and reaction. The occurrence of these spatially specific regions of decomposition or "hot spots" suggests that their origin is closely related to material microstructure and the associated plastic deformation and fracture properties of the energetic material being studied.

As early as the Fourth Symposium (International) on Detonation, which was held in 1965 in cooperation with the Office of Naval Research, Green and James[2] reported small-scale gap test results, indicating that crystalline explosives have important microstructural properties that directly influence their energetic properties. The degree of crystalline perfection of cyclotetramethylenetetranitramine (HMX) in 85/15 HMX/Viton formulations was found to strongly affect shock sensitivity. The explosive containing the higher quality HMX crystals was less shock sensitive.

Recent work to better understand the microstructural basis for hot spot phenomena has focused[3-8] on investigating the deformation and cracking behaviors of cyclotrimethylene-trinitramine (RDX) single crystals, primarily using microindentation hardness testing[9,10] techniques. In addition to being a widely used U.S. military explosive, RDX was selected because it is one of a number of materials exhibiting ignition essentially coincident with mechanical failure, as demonstrated in the drop-weight impact results reported by Heavens and Field.[11] The pressure-time curve for granular RDX showed a sharp drop with the pressure falling to zero. Ignition occurred almost simultaneously with the sharp drop in pressure. Connecting with these observations, the microhardness results indicate that the

plastic deformation is very inhomogeneous in RDX. Highly localized strain fields centered on the indentations were observed[2] by an etch pitting technique[12] and subsequently confirmed[5,8] by surface reflection Berg-Barrett x-ray topography[13,14] observations.

More recently, the initial stages of chemical decomposition in impacted production-grade RDX crystals has been studied in some detail.[6,7,15] Quantitative gas chromatographic results revealed the formation of two nitroso compounds, as solid-state decomposition products, in the "RDX residues" recovered from drop-weight impact tests. The important observation was made[6,15] that R-salt, the trinitroso analog of RDX (a known[16] decomposition product in thermally degraded RDX) was formed. This occurred in samples that were impacted not only at energy levels sufficient to cause the evolution of hot decomposition gases but also at lower energy levels that resulted only in the occurrence of hot spots, as detected by a heat sensitive film[17] technique.

Observations on the drop-weight impact behavior of granular ammonium perchlorate (AP) were also made by Heavens and Field.[11] The AP response was similar to RDX. A sharp drop occurred in the pressure-time curve, but the magnitude of the pressure did not diminish to zero. Ignition was also essentially coincident with the sharp drop in pressure. Some initial microindentation hardness results were obtained by Yoo and Rosemeier[6] on a high quality, pure single crystal of AP supplied by T. Boggs, Naval Weapons Center (NWC), China Lake, CA. A substantial hardness anisotropy was measured, but it was not as pronounced as has been obtained[3-5,8] for RDX. Unpublished surface reflection Berg-Barrett topographs revealed that the strain fields around the hardness impressions were not as localized either.

The properties of dislocations in AP are important in understanding its plastic deformation and fracture behaviors. Further, dislocations are proposed to be involved in the formation of hot spots in crystalline energetic materials.[3-8] Two groups of researchers have studied the properties of dislocations in AP single crystals. Using optical and transmission electron microscopy, Herley, Jacobs, and Levy[18] successfully identified a number of slip planes and slip directions. This was accomplished by analyzing the plane traces produced by dislocation etch pit arrays on crystals that had been tested in compression. The traces were observed on the (210) and (001) cleavage surfaces. Additional study of the cleavage and growth faces of AP crystals that had been deformed has been described by Williams, Thomas, Savintsev, and Boldyrev.[19] Interference-contrast microscopy was used to examine etch pit arrays and slip traces. The crystals were deformed in compression and by indenting with a sharp needle. Many of the slip planes and slip directions reported by Herley, Jacobs, and Levy were identified, along with a number of additional slip planes. The drop-weight impact result obtained by Heavens and Field[11] for AP is surprising, for one reason, because the total

results obtained from the previously described, slow rate deformation studies on RDX and AP show that AP is considerably more ductile.

The chemical reactivity of AP has been studied extensively because of its widespread use as an oxidizer in solid propellants. The heat of reaction for AP is low (405 cal/g; Reference 20) relative to high explosives, but pressed AP can be made to detonate[21] in the NOL Large Scale Gap Test when the charge density does not exceed approximately 80% theoretical maximum density (%TMD). Thus, it is possible to conclude that AP reacts when shocked but sample defects are necessary to achieve rapid growth of reaction. This suggests the feasibility of studying, perhaps on a microscopic scale, the role that defects have in enhancing shock reactivity in AP. In addition to the small-scale gap test results[2] mentioned previously for HMX/Viton formulations, Dick[22] reported that microscopic damage resulting from exposure to gamma radiation enhanced the shock sensitivity of pentaerythritol-tetranitrate (PETN) single crystals. Also for PETN, the shock sensitivity of a relatively defect-free crystal is a function of its orientation, leading Dick[23] to conclude that shock-induced defects depend on lattice arrangement.

The threshold for shock-induced reaction in AP samples pressed to 87% TMD was initially studied by Macek and Durfee[24] about 20 years ago. The samples were sealed in polyvinyl dichloride, and an ingenious recovery technique was developed so that the samples often remained sealed after the shock experiments. This permitted the determination of the amount of gaseous decomposition products from weight loss measurements. The onset of reaction was detected to occur at about 9 kbar for a 12 μs duration shock and at about 5 kbar for a 21 μs duration shock.

In the current work, the chemical reactivity of AP single crystals, supplied by T. Boggs, NWC, subjected to mechanical deformation, particularly relating to low amplitude shock waves is being studied in detail. Of special interest are the roles that mechanical deformation and consequent material microstructure have on the shock reactivity of AP. Results are being obtained on the following issues:

(1) the crystal deformation properties;
(2) the deformed crystal microstructures;
(3) the shock wave characteristics required for crystal initiation; and
(4) the chemical state of shocked crystals.

The work builds directly on the previously described research results obtained by other investigators and involves a closely allied effort between researchers at Loyola College, Baltimore, the Naval Surface Warfare Center (NSWC), White Oak Laboratory, and the University of Maryland, College Park. Microindentation hardness testing of an AP single crystal was performed at Loyola

College along with an examination of the residual hardness impressions using polarized light microscopy. A number of shock wave experiments were conducted at NSWC on pressed AP pellets and single crystals. Quantitative chemical analyses, using liquid ion chromatography, were obtained at NSWC on some of the samples that had been shocked. The results from these investigations that have been achieved to date are described in the sections that follow in this report.

STEREOGRAPHIC PROJECTION DESCRIPTION OF PREVIOUSLY IDENTIFIED SLIP SYSTEMS IN AP

The stereographic projection displays in two dimensions the angular relationships between crystallographic planes and directions. Planes appear as great circle lines, and directions and plane normals are represented as points. As such, the stereographic projection provides a convenient way to show slip system information. The slip plane normals (SP) and slip directions (SD) identified from plane traces (T) by previous researchers[18,19] appear in Figure 1. The combined results are shown on a $(\bar{2}\bar{1}0)$ stereographic projection since the $(\bar{2}\bar{1}0)$ surface is prominently displayed in the next figure of the AP single crystal investigated in this work.

ORIENTATION OF CLEAVED AP CRYSTAL

A scale drawing of the cleaved AP crystal initially chosen for study appears in Figure 2. This crystal was chosen in part because two of its exposed cleavage surfaces, the $(\bar{2}10)$ and (001) planes, are orthogonal to one another. This condition permitted both surfaces to undergo microindentation hardness testing without having to mount the crystal. The crystal appeared to be of very good quality as it was perfectly optically transparent.

A Laue back reflection photograph was obtained with the x-ray beam directed normal to what was determined to be the $(\bar{2}10)$ surface. Polaroid Type 57 film was placed 3 cm from this surface which was then exposed to CuKα radiation at 20 kV and 15 mA for 1 h. The spots on the photograph were sharp, indicating good perfection in small volumes of the crystal. The film was read through its back in order to identify various planes and directions that emanate from the $(\bar{2}10)$ surface. A zone analysis was performed allowing identification of the $(\bar{2}10)$ surface as viewed directly. A schematic representation of the Laue photograph that was analyzed appears in Figure 3, where a number of prominent zones and their axes are identified. Surprisingly,

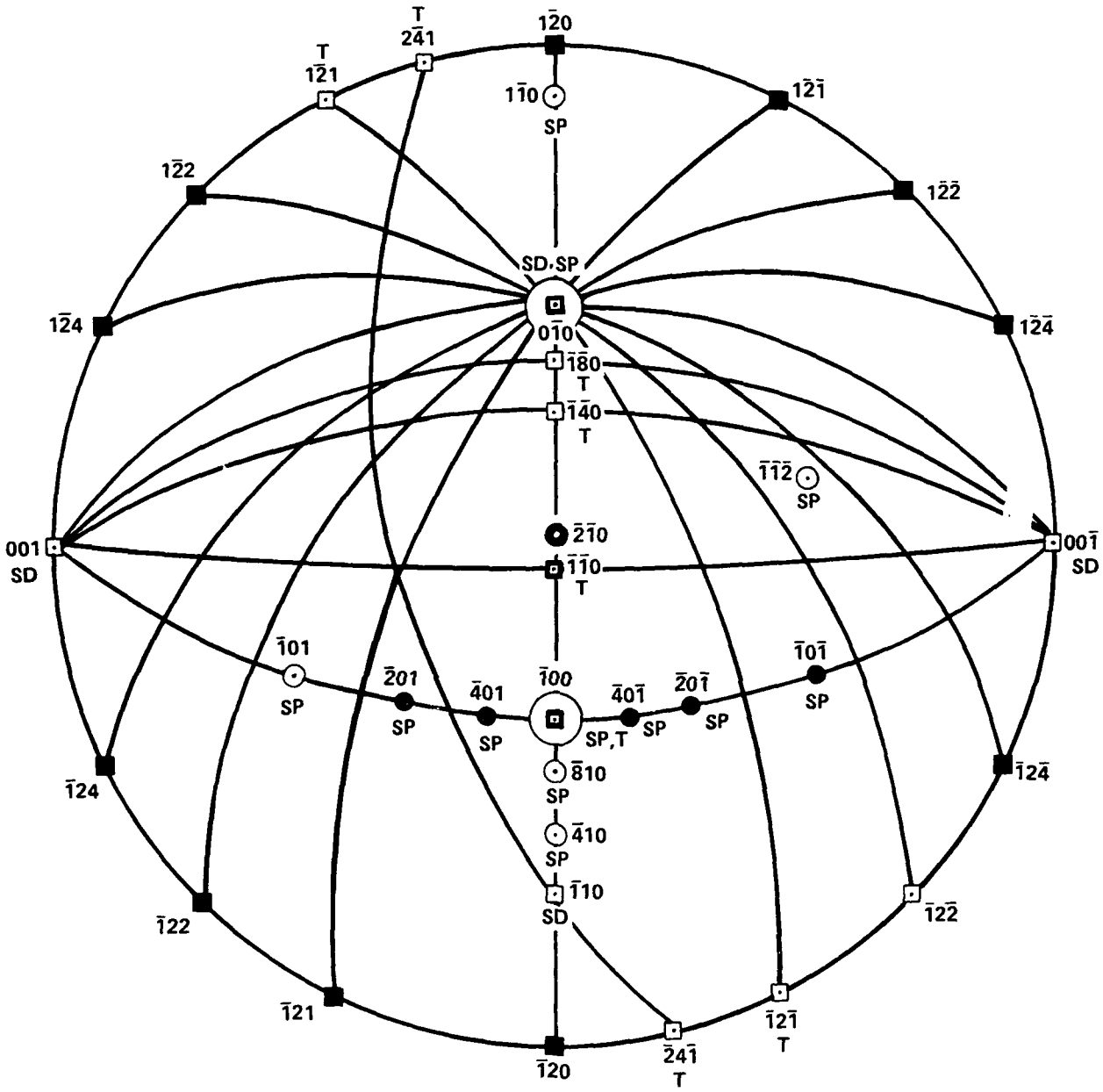

⊙, PLANE NORMALS, AND ⊡, DIRECTIONS: HERLEY, JACOBS, AND LEVY
●, PLANE NORMALS, AND ■, DIRECTIONS: WILLIAMS, THOMAS, SAVINTSEV, AND BOLDYREV

FIGURE 1. $(\bar{2}\bar{1}0)$ STEREOGRAPHIC PROJECTION FOR AMMONIUM PERCHLORATE SHOWING PREVIOUSLY REPORTED SLIP SYSTEMS AND THEIR TRACES

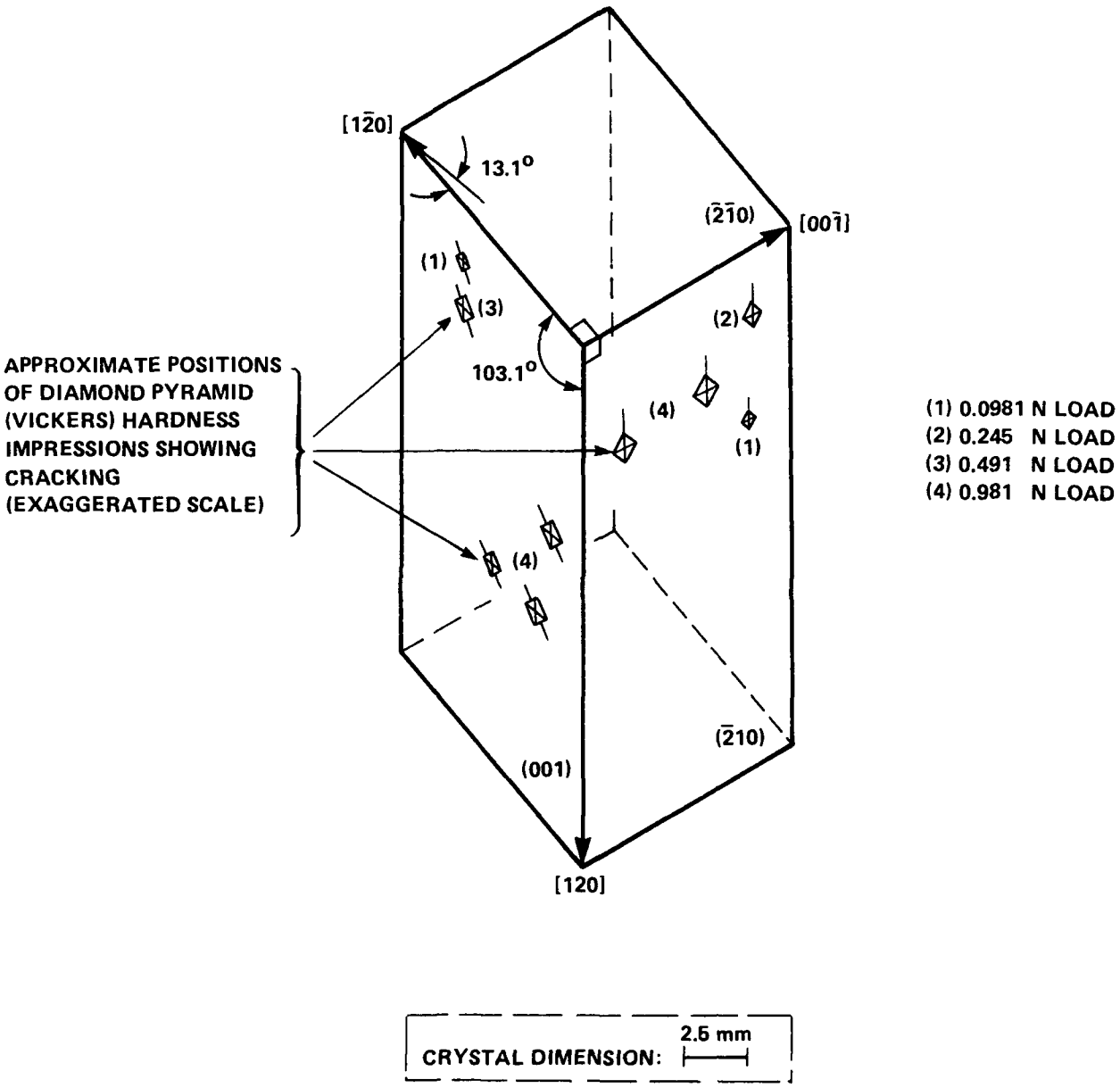

FIGURE 2. SCALE DRAWING OF CLEAVED AMMONIUM PERCHLORATE SINGLE CRYSTAL USED IN MICROINDENTATION HARDNESS TESTS

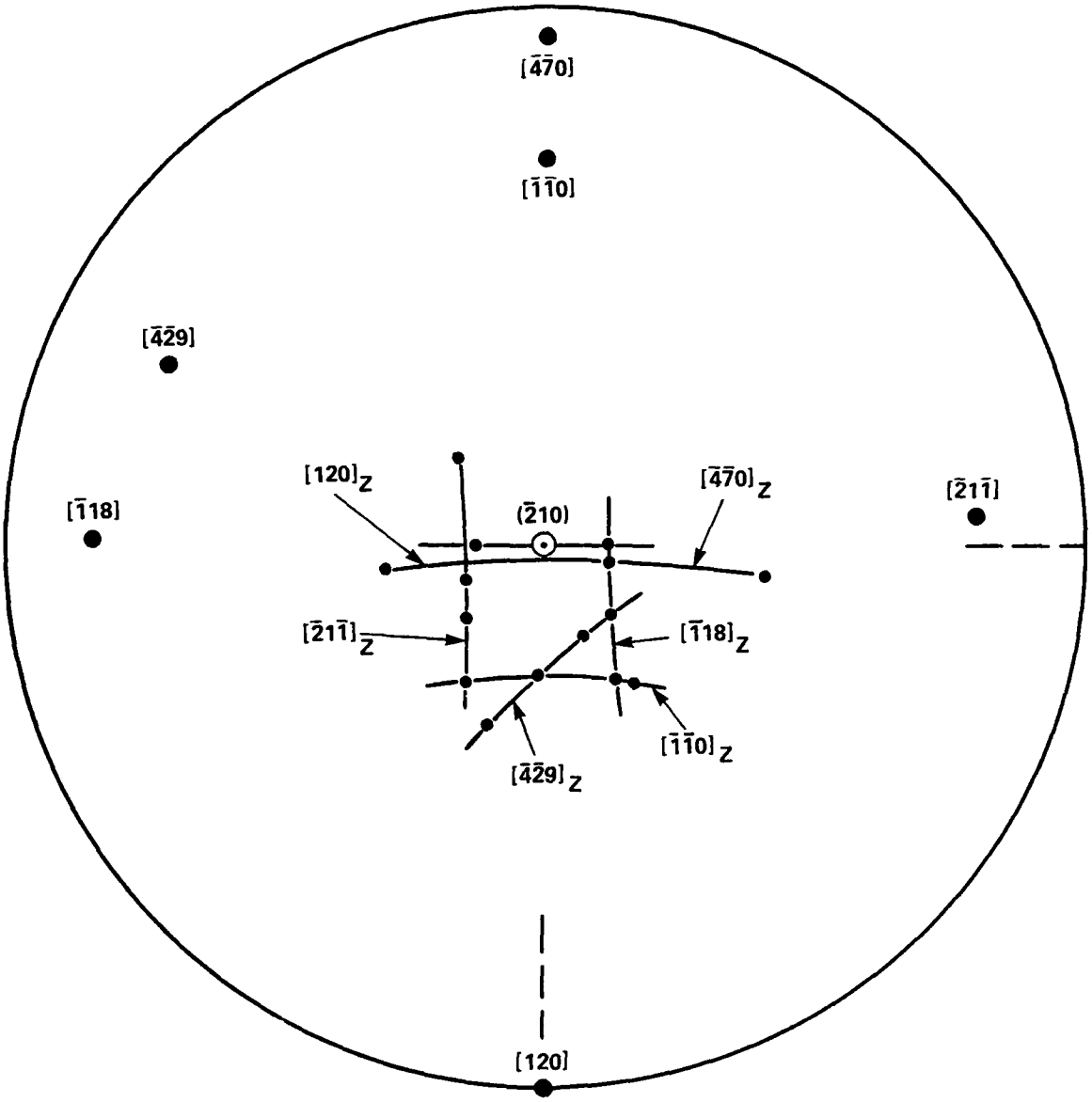

FIGURE 3. BACK REFLECTION LAUE PHOTOGRAPH IN COMBINATION WITH STEREOGRAPHIC PROJECTION SHOWING ZONES OF DIFFRACTION SPOTS AND ZONE AXES TO IDENTIFY THE ($\bar{2}10$) SURFACE OF AMMONIUM PERCHLORATE AS DIRECTLY VIEWED

a number of the zones had high indices. To confirm this analysis, a second Laue back-reflection photograph was obtained in which the x-ray beam was normal to the cleavage surface that was orthogonal to the $(\bar{2}10)$ surface. This photograph was independently analyzed resulting in the identification of the (001) surface as expected. A number of prominent zones in the second Laue photograph also had high indices.

COMPUTER-GENERATED STEREOGRAPHIC PROJECTIONS FOR AP

The structural information provided in Figures 1 and 2 was determined using the $(\bar{2}10)$ stereographic projections for AP appearing in Figures 4 and 5, where plane normals and directions are separately displayed, respectively. Additional information is provided in the (001) stereographic projections for AP appearing in Figures 6 and 7. Previous efforts by Kosel[25,26] and Staley[27,28] in constructing computer-generated stereographic projections for other materials have been adapted for use with an IBM PC/XT computer system and a Hewlett-Packard Laser Jet II letter-quality printer to obtain the projections shown (redrawn) in this report. The projections were obtained by separately calculating the angles between planes and then directions, given the dimensions,[29] a = 9.231 Å, b = 5.813 Å, c = 7.453 Å, of the orthorhombic unit cell for AP. In constructing Figures 4 to 7, only the indices that are no higher than 2 were included. The plane normals and crystal directions are not coincident for the non-cubic AP crystal structure. The plane normal and direction plots are shown separately, in order to simplify the presentation of the information given.

INITIAL MICROINDENTATION HARDNESS STUDY OF THE DEFORMATION IN AP

To assess the plastic deformation and fracture behaviors of AP in a controlled way, microindentation hardness testing was employed. Both the $(\bar{2}10)$ and (001) cleavage surfaces were indented several times with a diamond pyramid (Vickers) indenter using loads ranging from 0.0981 to 0.981 N (Figure 2). The residual impressions were then studied using transmitted light, reflected light, and polarized transmitted light microscopy. Nomarski interference contrast microscopy was also performed. An example of the hardness impressions that were put into each of the surfaces has been chosen for the discussion that follows.

The transmitted light micrograph in Figure 8(A) shows a diamond pyramid (Vickers) indentation (0.981 N load) put into the

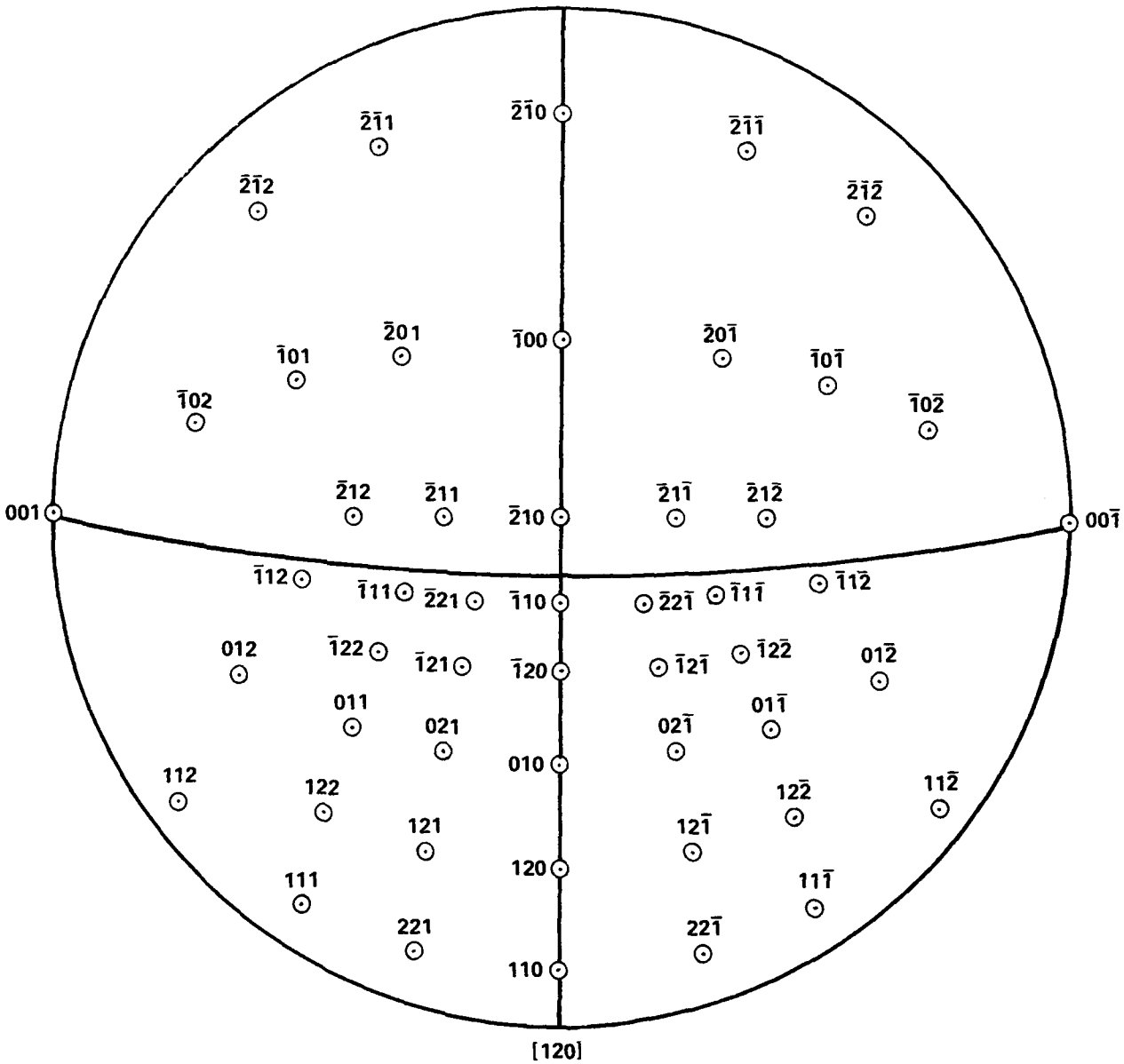

FIGURE 4. STANDARD ($\bar{2}10$) PROJECTION FOR AMMONIUM PERCHLORATE SHOWING PLANE NORMALS

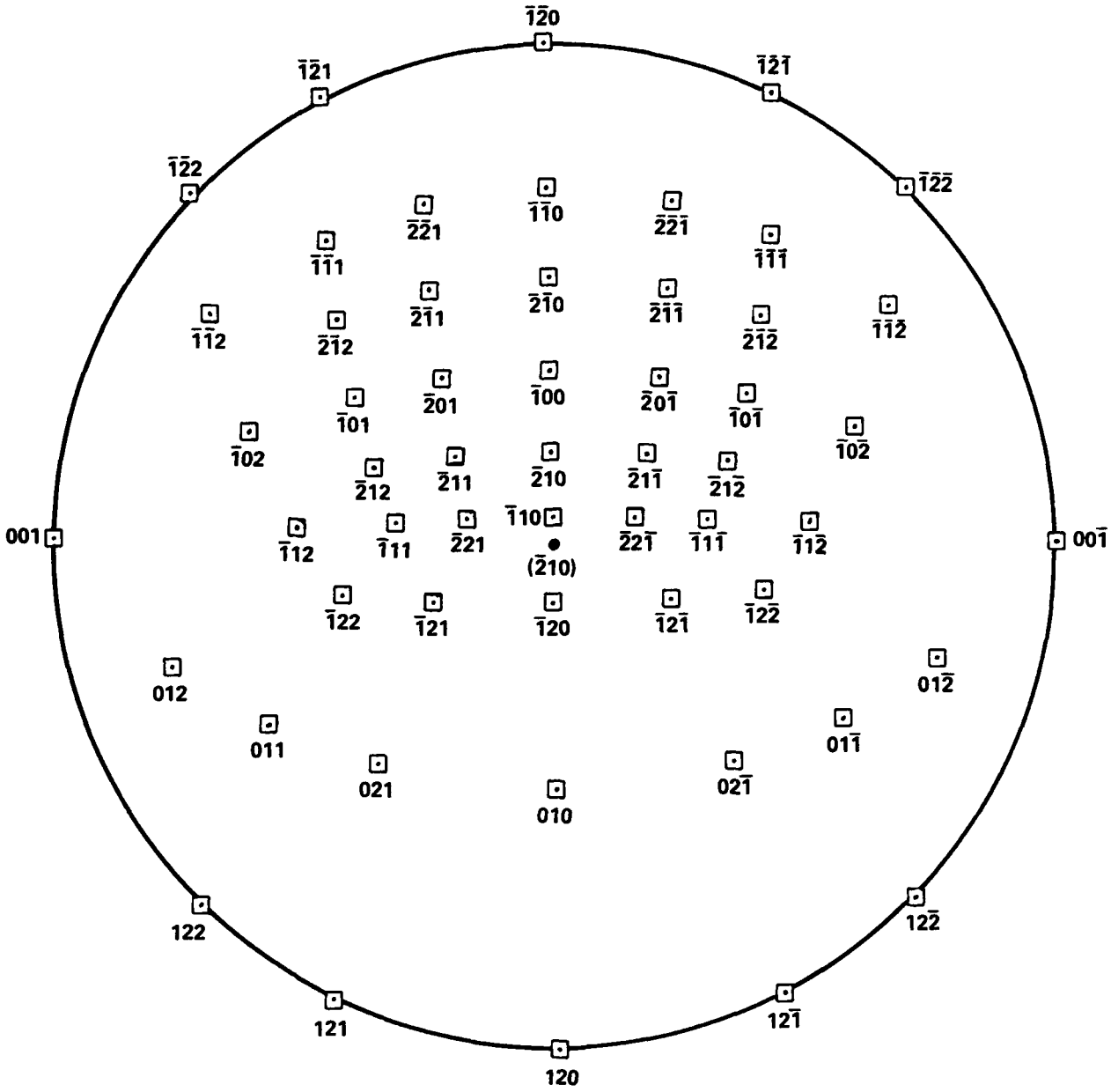

FIGURE 5. STANDARD ($\bar{2}10$) PROJECTION FOR AMMONIUM PERCHLORATE SHOWING DIRECTIONS

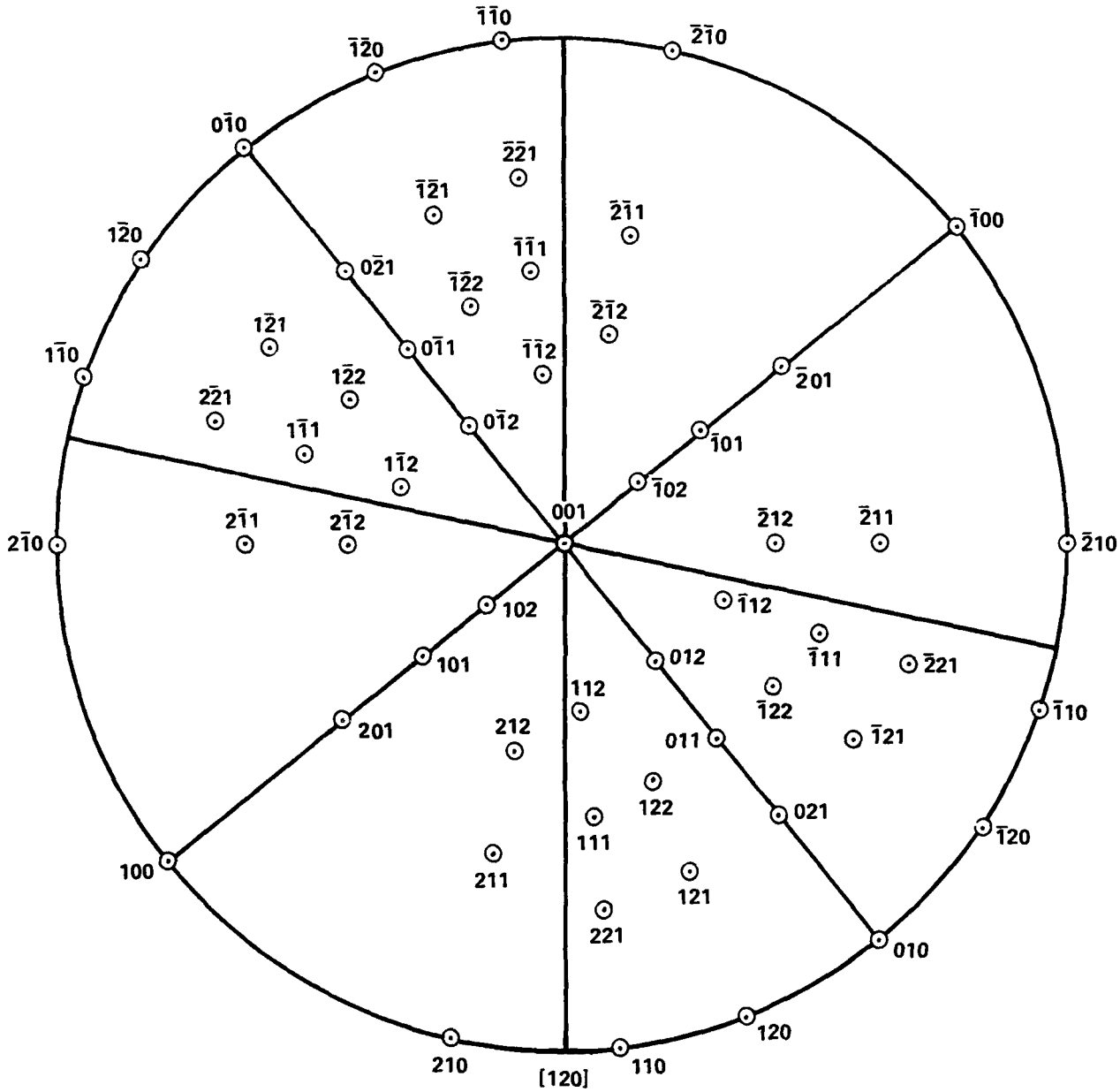

FIGURE 6. STANDARD (001) PROJECTION FOR AMMONIUM PERCHLORATE SHOWING PLANE NORMALS

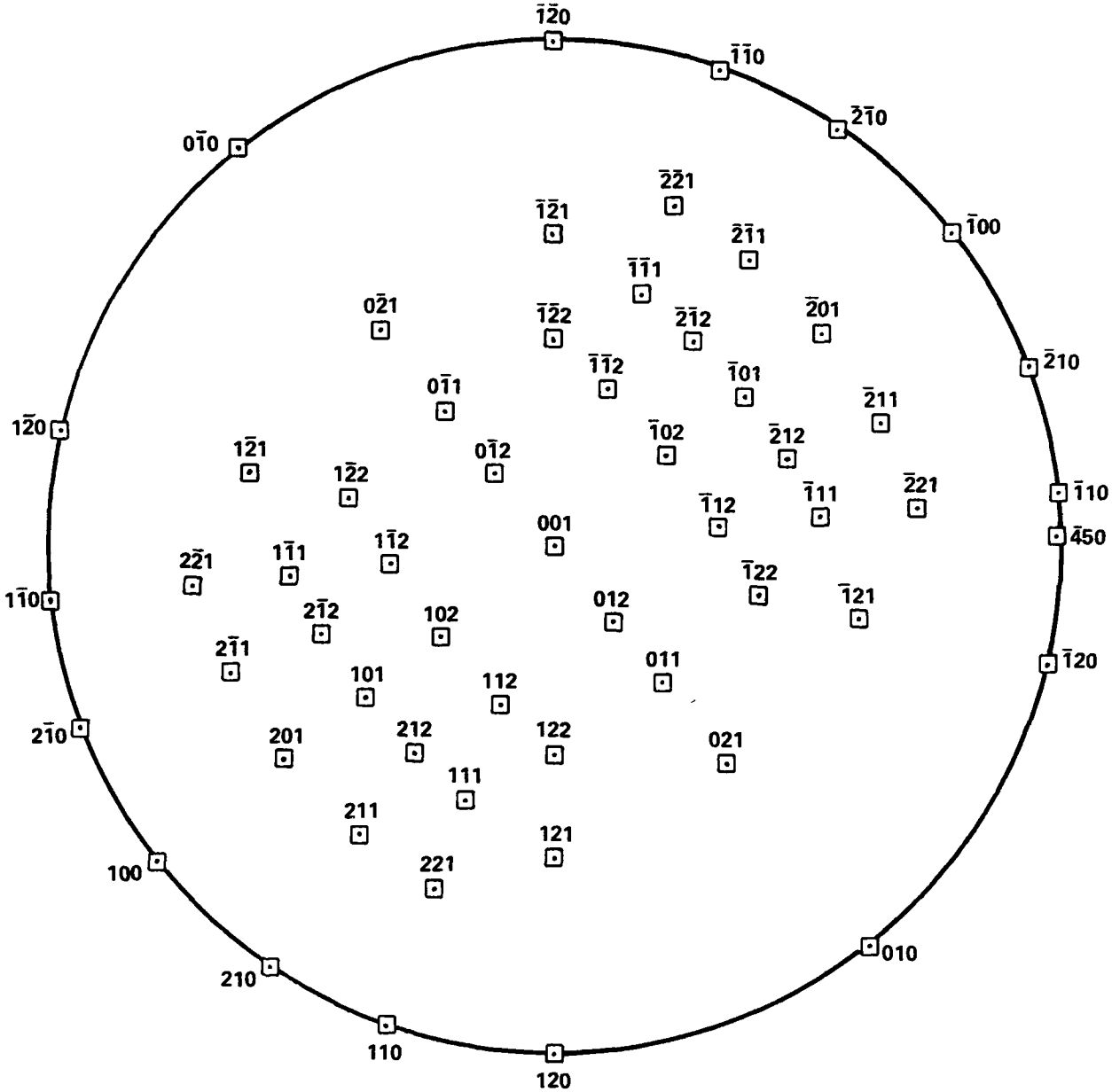

FIGURE 7. STANDARD [001] PROJECTION FOR AMMONIUM PERCHLORATE SHOWING DIRECTIONS

(A) TRANSMITTED LIGHT

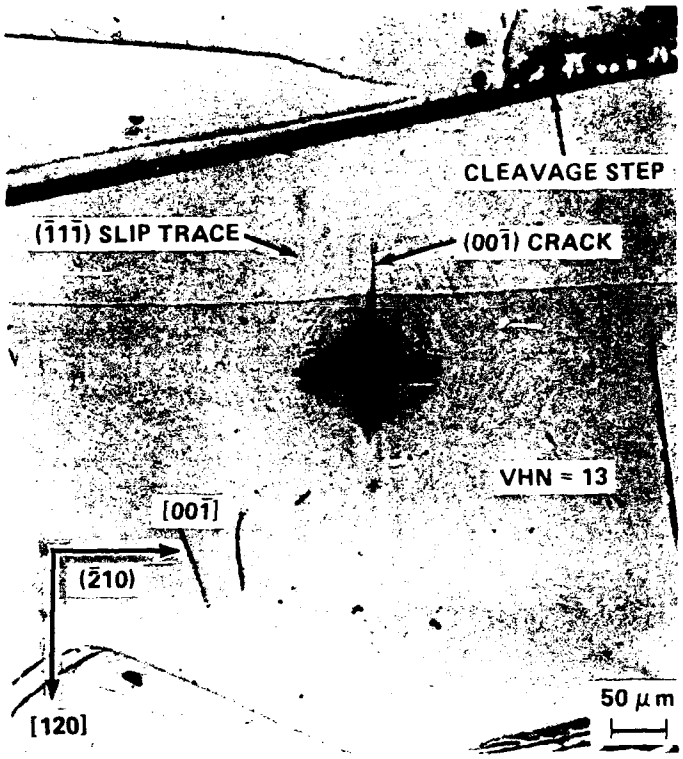

(B) POLARIZED LIGHT

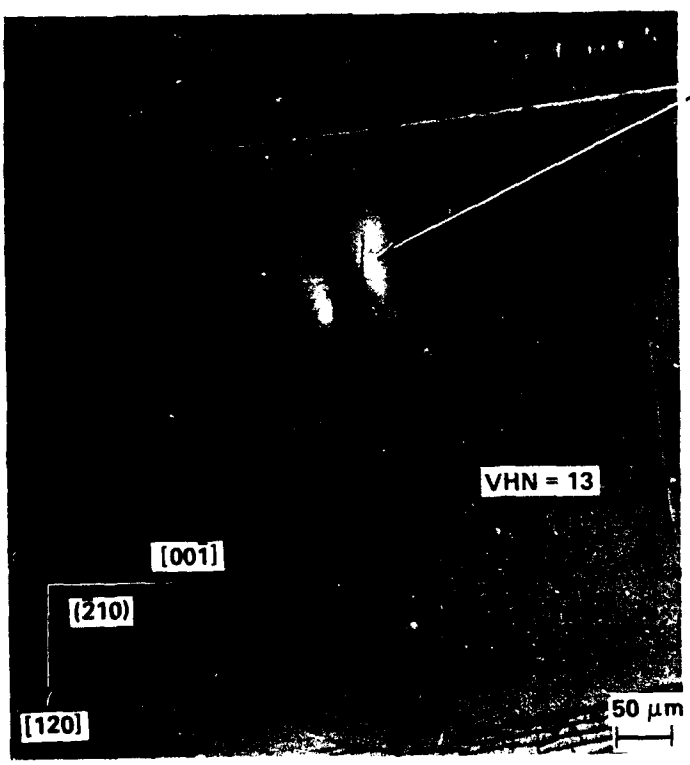

FIGURE 8. DIAMOND PYRAMID (VICKERS) HARDNESS IMPRESSION IN (2̄10) SURFACE OF AMMONIUM PERCHLORATE VIEWED IN (A) TRANSMITTED LIGHT AND (B) POLARIZED LIGHT

($\bar{2}10$) surface of AP. The Vickers hardness number (VHN) of 13 kgf/mm^2 (127 MPa) indicates that AP is soft, only 1/3 to 1/2 the hardness of the molecular crystalline explosive RDX, for example. The indentation is asymmetrically formed even though care was taken to level the indented surface so that it was normal to the indenter axis. The asymmetry is caused by a difference in the operative slip systems available to form the impression. As viewed, more extensive primary plastic deformation has occurred above the [00$\bar{1}$] direction in accommodating the two upper facets of the indenter. Considerable secondary plastic deformation corresponding to the slip traces that frame the indentation is also clearly evident. For example, a slip trace that develops when the ($\bar{1}1\bar{1}$) plane becomes displaced at the ($\bar{2}10$) surface is identified. In addition, slip-induced (00$\bar{1}$) cleavage cracking is involved in putting the indentation into the surface. Additional information on the operative deformation systems involved in forming the impression is given in subsequent discussion.

When the hardness impression is viewed between cross polarizers rotated to provide maximum extinction, transmitted light is observed (Figure 8(B)). In a polarized light study of glide bands in NaCl single crystals, Mendelson[30] attributed the occurrence of transmitted light to edge dislocation arrays. The transmitted light in Figure 8(B) is observed to occur in the region of the indentation that has undergone the most extensive plastic deformation. Also, the transmitted light extends considerably beyond the furthermost tip of the (00$\bar{1}$) cleavage crack. This suggests that the crack has not been completely successful in relieving the stress caused by the dislocation arrays. Further, the extent of the strain field, as evidenced by the transmitted light, is considerably larger than that observed for RDX hardness impressions studied by etch pitting[3] and surface reflection x-ray topographic[5,31] techniques. As such, the plastic deformation is not nearly so localized in AP as compared to RDX, which exhibited extremely localized deformation zones around hardness impressions.

The transmitted light micrograph in Figure 9(A) shows a diamond pyramid hardness impression (0.981 N load) in the (001) surface of AP. A slightly lower hardness pressure, VHN = 11 kgf/mm^2 (108 MPa), was measured compared to the value of 13 kgf/mm^2 obtained for the ($\bar{2}10$) surface. The four facets of the impression in Figure 9(A) have a distorted 4-fold rotational symmetry. The four segments of the perimeter formed at the exterior (001) surface are wavy, and small cracks are present in this perimeter region. Much larger cracks are observed to emanate from two sides of the impression. To date, these cracks have not been definitively identified. Slip in the [001] direction spreading along $\pm$[010] on $\pm$($\bar{1}$00) planes is responsible for the traces at the facet edges parallel to $\pm$[010]. As such, the (100)[001] slip system is the primary deformation system involved in forming the impression, as will be described in subsequent discussion. Perhaps surprisingly, the (001)[010] slip system could have been involved in forming facets with edges

(A) TRANSMITTED LIGHT

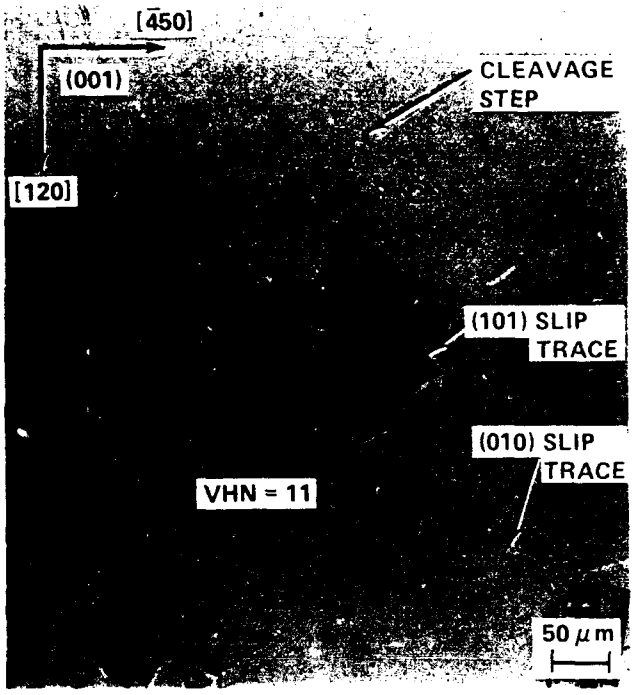

(B) POLARIZED LIGHT

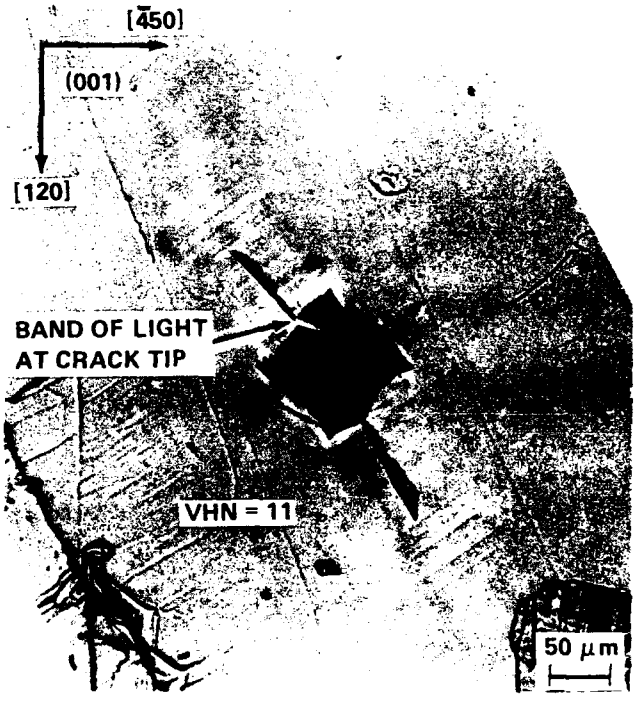

FIGURE 9. DIAMOND PYRAMID (VICKERS) HARDNESS IMPRESSION IN (001) SURFACE OF AMMONIUM PERCHLORATE VIEWED IN (A) TRANSMITTED LIGHT AND (B) POLARIZED LIGHT

along $\pm[100]$. Prominent $\pm(010)$ slip traces of limited extent, but occurring at large distances from the indentation, are proposed to form as a result of the secondary plastic deformation process. In addition, secondary slip on (101) has been labeled in Figure 9(A) as occurring outside of the primary indentation forming deformation field.

When viewed in polarized light (Figure 9(B)), the impression in the (001) surface yielded significantly less transmitted light compared to the impression in the $(\bar{2}10)$ surface. With the cross polarizers oriented to provide maximum extinction, the most obvious feature is a bright, sharply focused band of light near the impression at the tip of one of the cracks. This suggests that considerable strain energy is stored in the vicinity of this crack tip. Transmitted light was also observed close to the corners of the hardness impression. However, there was a surprising absence of transmitted light in the surrounding region away from the hardness impression. Rotating the AP crystal about the [001] direction relative to the polarization direction in the cross-polarizer did not appear to alter this finding. This observation suggests that the strain energy around the residual impression is localized, although extensive secondary plastic deformation has occurred. Perhaps the explanation lies in the role that the cracking has in dissipating the strain energy.[32] The strain fields around the hardness impressions will be investigated using Berg-Barrett surface reflection x-ray topography to elucidate further the result.

The hardness impressions put into AP were also interesting for the surface relief that was observed. Figure 10 shows hardness impressions viewed in transmitted light that was partially obstructed before the light entered the crystal. A shadow effect resulted that allowed a very shallow trough to be observed (Figure 10(A)) to extend in the $\pm[00\bar{1}]$ directions far away from the impression in the $(\bar{2}10)$ surface. Prominent deep troughs were found (Figure 10(B)) to emanate from the impressions in the (001) surface. The surface relief that occurs in forming hardness impressions in AP is somewhat analogous to observations[33] for impressions in MgO. A schematic view of the surface relief and {011} cracking caused by dislocation motion and interactions in the rocksalt crystal structure is shown in Figure 11.

The $(\bar{2}10)$ hardness impression and consequent deformation plane traces are shown on the associated indentation drawing and stereographic projection that appear in Figure 12. The $(00\bar{1})$ crack near to the intersection of adjacent facets 1 and 2 in the indentation drawing is shown schematically along the top half of the vertical diameter of the stereographic projection. As much as possible, the reference slip system information[18,19] provided in Figure 1 has been utilized in determining the deformation systems chosen to explain the current hardness results. For example, the relative position of the easy $(\bar{1}00)[010]$ slip system, compared to $(010)[\bar{1}00]$, leads to the expectation that

(A) ($\bar{2}10$) SURFACE

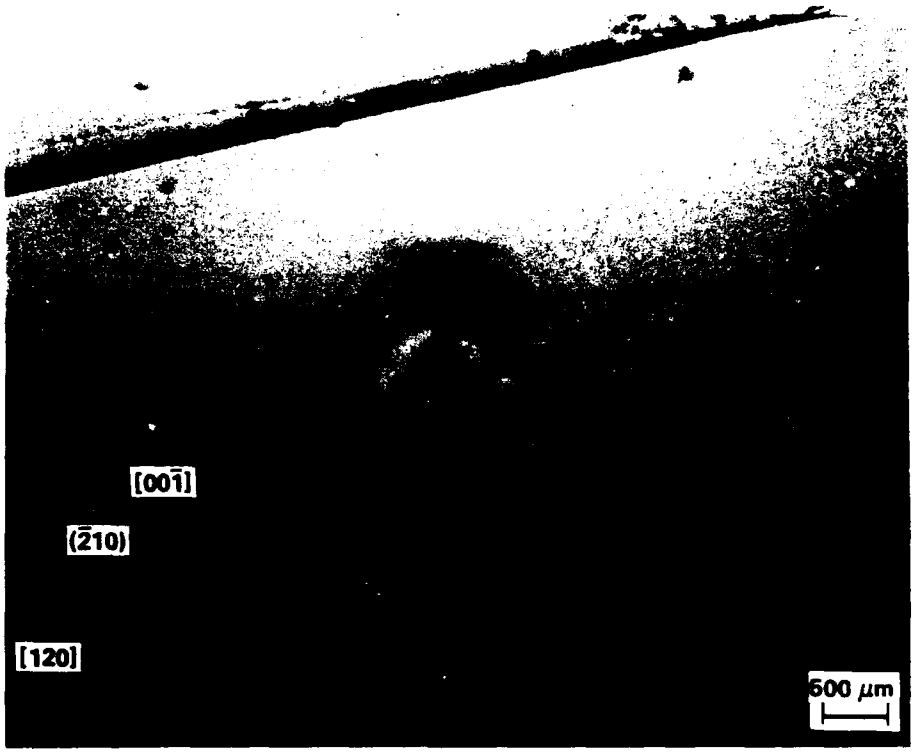

(B) (001) SURFACE

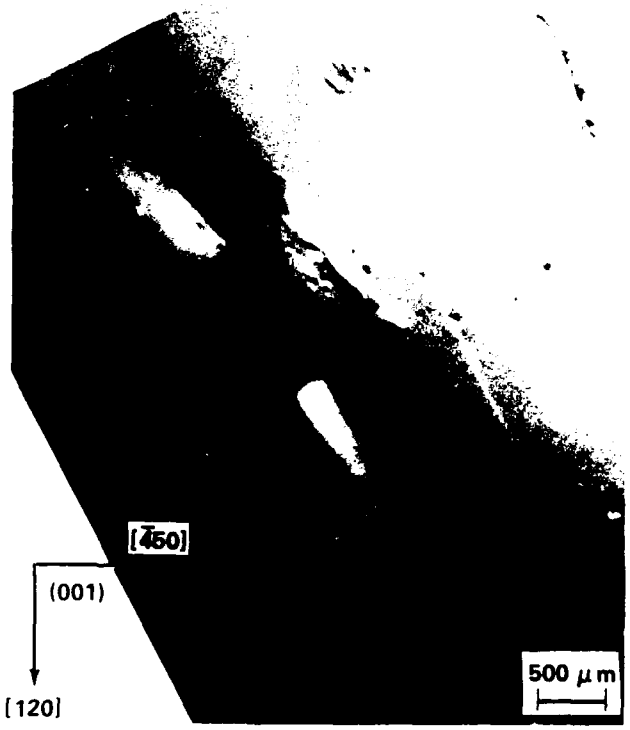

FIGURE 10. DIAMOND PYRAMID (VICKERS) HARDNESS IMPRESSION IN (A) ($\bar{2}10$) SURFACE AND (B) (001) SURFACE OF AMMONIUM PERCHLORATE VIEWED IN PARTIALLY OBSTRUCTED TRANSMITTED LIGHT TO REVEAL SURFACE RELIEF

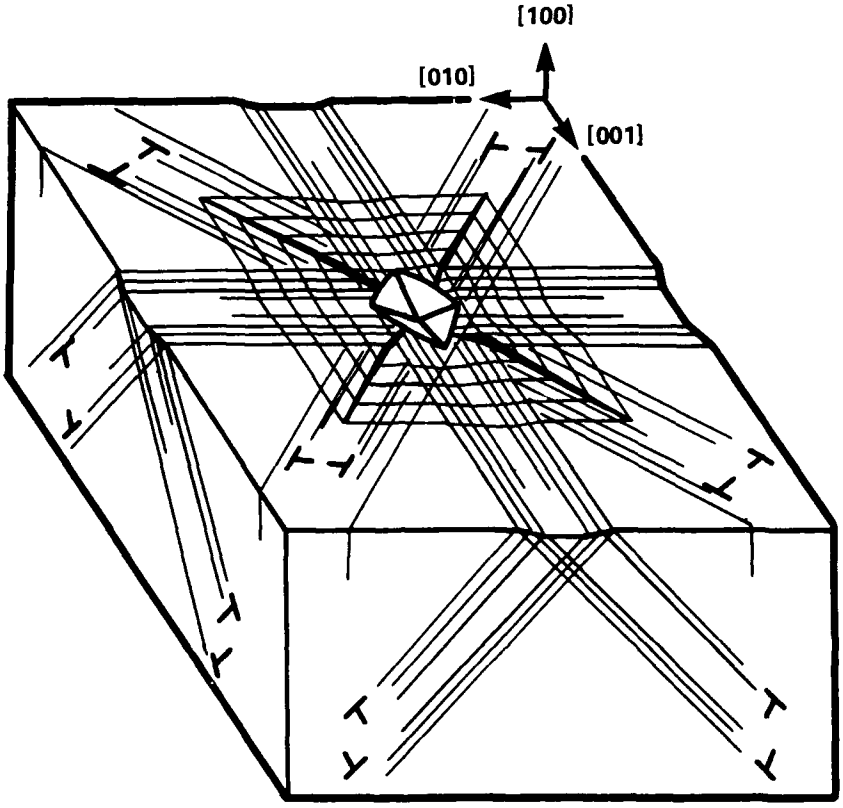

[001] DIAGONAL ANALOG OF [011] DIAGONAL IMPRESSION:
ARMSTRONG AND WU [33]

FIGURE 11. DISLOCATION MODEL APPLIED TO SLIP TRACES AT [001] DIAGONAL DIAMOND PYRAMID (VICKERS) HARDNESS IMPRESSION IN THE ROCKSALT CRYSTAL STRUCTURE

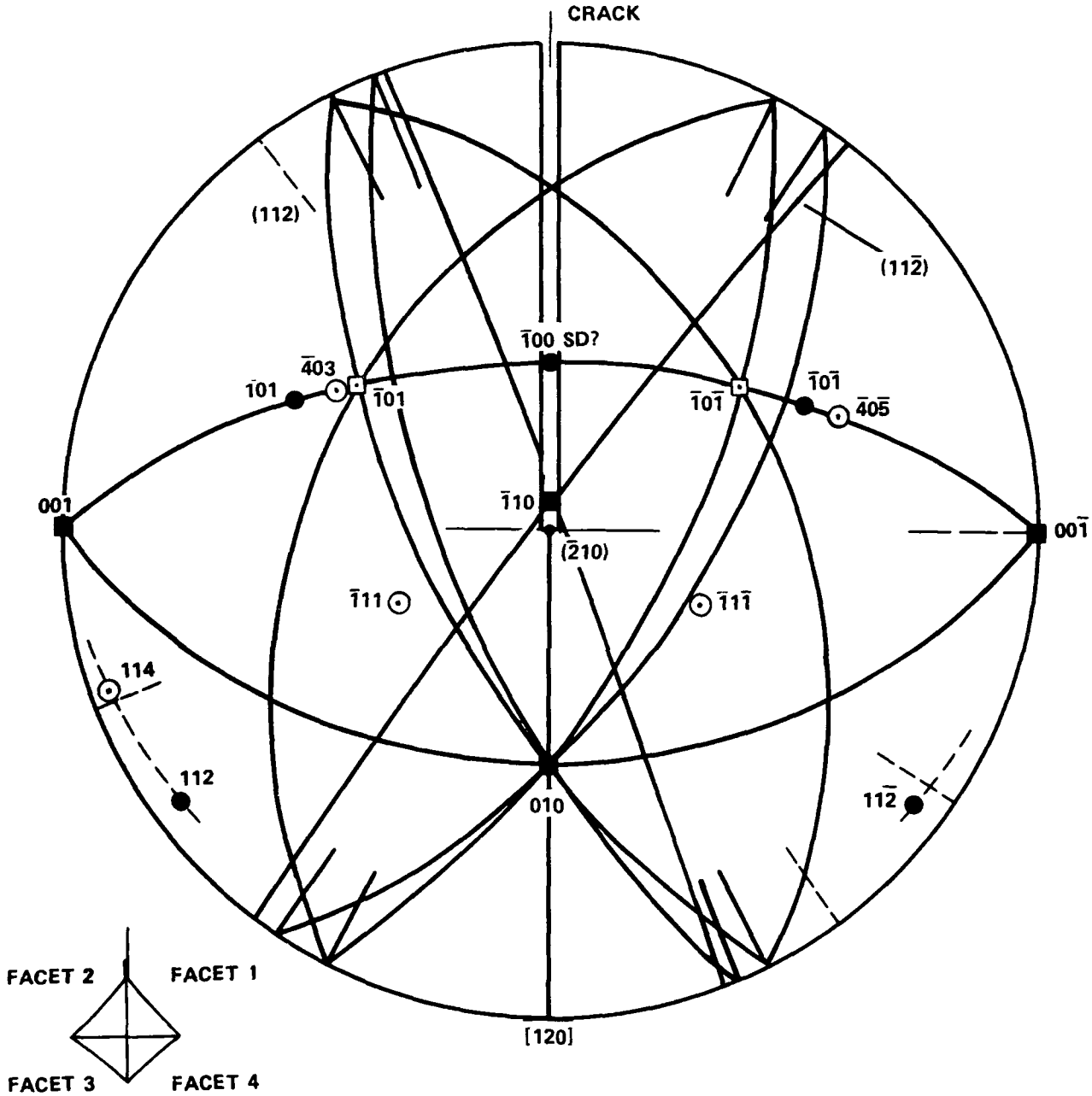

⊙, ●, PLANE NORMALS, AND ⊡, ■, DIRECTIONS
CLOSED SYMBOLS DENOTE REPORTED SLIP SYSTEMS [18, 19]

FIGURE 12. STEREOGRAPHIC PROJECTION SHOWING DEFORMATION SYSTEMS FOR DIAMOND PYRAMID (VICKERS) HARDNESS IMPRESSION IN ($\bar{2}$10) SURFACE OF AMMONIUM PERCHLORATE

facets 1 and 2 should be larger than facets 3 and 4. Other slip systems which could be involved for facets 1 and 2 are $(\bar{1}0\bar{1})[010]$ and $(\bar{1}01)[010]$, respectively, and $(\bar{1}00)$, $\pm[00\bar{1}]$. Facets 3 and 4 are possibly accounted for by relatively difficult slip on $(\bar{1}11)[\bar{1}0\bar{1}]$ and $(\bar{1}1\bar{1})[\bar{1}01]$, respectively. Slip on the (010), $\pm[00\bar{1}]$ system could be operative for both facets, but this seems improbable on the basis that this sole reported slip direction is in the indented $(\bar{2}10)$ surface. Although $[\bar{1}00]$ slip on (010) seems to be a geometrically favorable system, it was previously inferred[18] as being unlikely. The possibility of $(010)[\bar{1}00]$ slip or slip on another system with a component normal to the $(\bar{2}10)$ surface, such as $\{111\}\langle 101\rangle$, is necessary to explain the surface relief observed along $\pm[001]$ as shown in Figure 10(A). In addition, a component of slip on (001) in the [100] direction was reported by Williams, Thomas, Savintsev, and Boldyrev.[19]

Secondary slip systems are required to operate outside the indentation facets in order to minimize any volume change associated with the indentation process.[33] Such secondary slip is responsible for the "picture frame" appearance enclosing the [001] diagonal diamond pyramid indentation shown in Figure 11 for the rocksalt crystal structure. Although both primary (indentation forming) and secondary (indentation accommodating) slip is accomplished symmetrically with multiple $\{110\}\langle 1\bar{1}0\rangle$ slip systems for aligned indentations on {100} in rocksalt crystals, the operative secondary slip systems are not nearly so obvious for the aligned indentations on $(\bar{2}10)$ in Figures 8 and 10(A). Figure 13 gives a listing of the primary systems discussed above and also the secondary systems chosen to match the traces of slip systems clearly visible in Figure 10(A). Mostly new slip systems are apparently required to account for the secondary relief associated with facets 1 and 2. Cross-slip is proposed to be involved because of the variations measured among the individual traces and, also, because of their obvious waviness.

The strongly asymmetric indentation shown in Figures 9 and 10(B) for an otherwise aligned [120] diagonal indentation on (001) is an interesting case to analyze stereographically for the operative slip systems. Figure 14 shows the relevant indentation drawing and stereographic projection. Prominent troughs running along $\pm[010]$ from facets 2 and 4 appear to be associated with primary slip on the $\pm(100)[001]$ slip system. Secondary slip traces, even appearing relatively discrete or twin-like, are contained within the troughs and are attributed to the apparent $\pm(010)[001]$ slip system, which is orthogonal to [010]. The $(101)[010]$, $(\bar{1}01)[010]$, and $(100)[010]$ slip systems shown in the stereographic projection, though proposed to be operative primary systems for the $(\bar{2}10)$ indentation, would not be evident in Figure 9 because the slip displacements are in the plane of the surface. Also, these systems would not contribute to the apparent axes centered on $\pm[010]$ and $\pm[100]$ in (001) for the asymmetric indentation shape. A diamond pyramid indentation with diagonal aligned along $\pm[010]$ did show essentially two-fold rotational symmetry about [001]. However, the asymmetric cracking evident

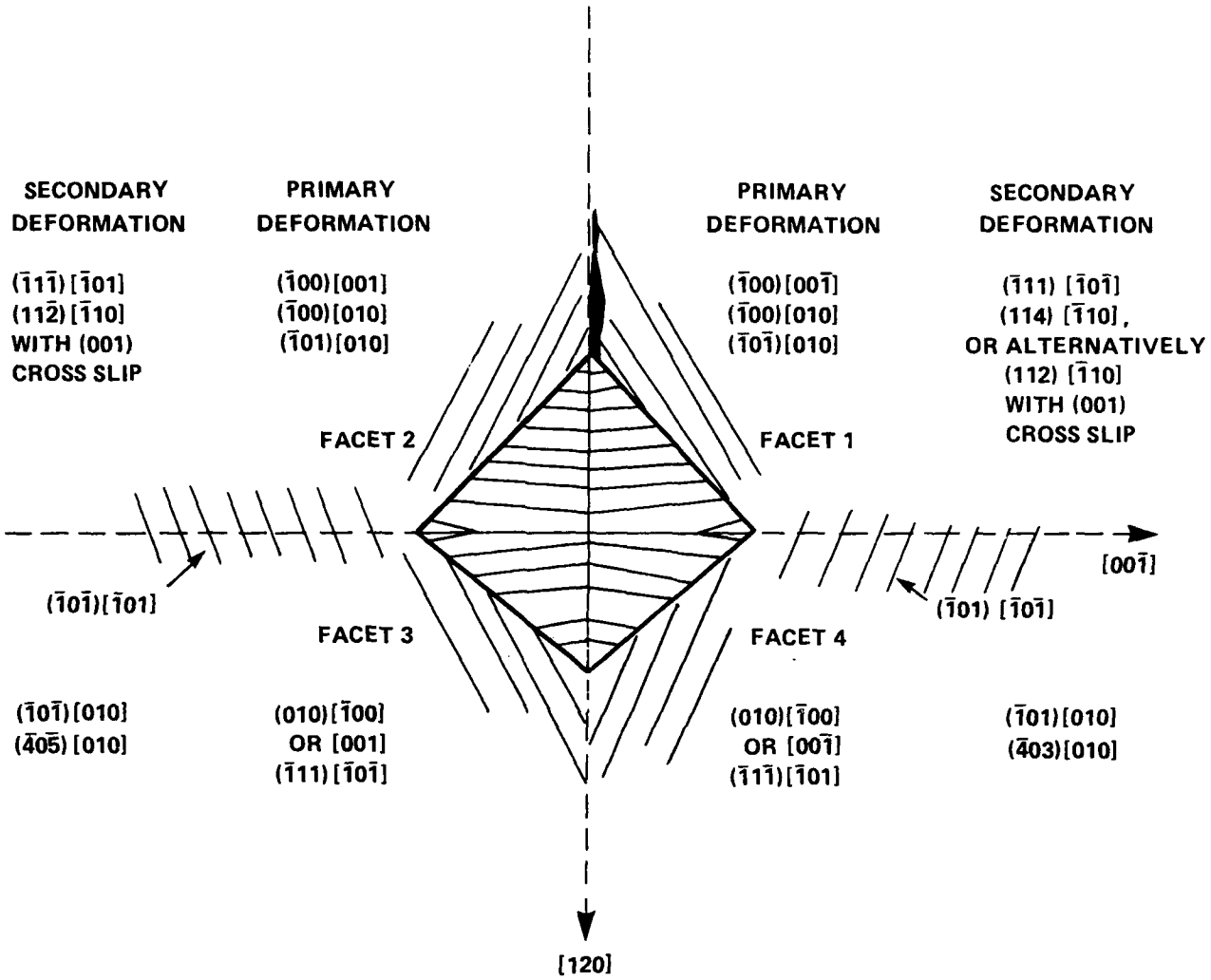

$$[\bar{1}0\bar{1}]_{(\bar{1}11)} + [10\bar{1}]_{(\bar{1}1\bar{1})} \longrightarrow [00\bar{2}]_{(00\bar{1})_C}$$

SLIP - INDUCED CLEAVAGE

FIGURE 13. PRIMARY AND SECONDARY DEFORMATION SYSTEMS INVOLVED IN FORMING DIAMOND PYRAMID (VICKERS) HARDNESS IMPRESSION IN THE ($\bar{2}$10) SURFACE OF AMMONIUM PERCHLORATE

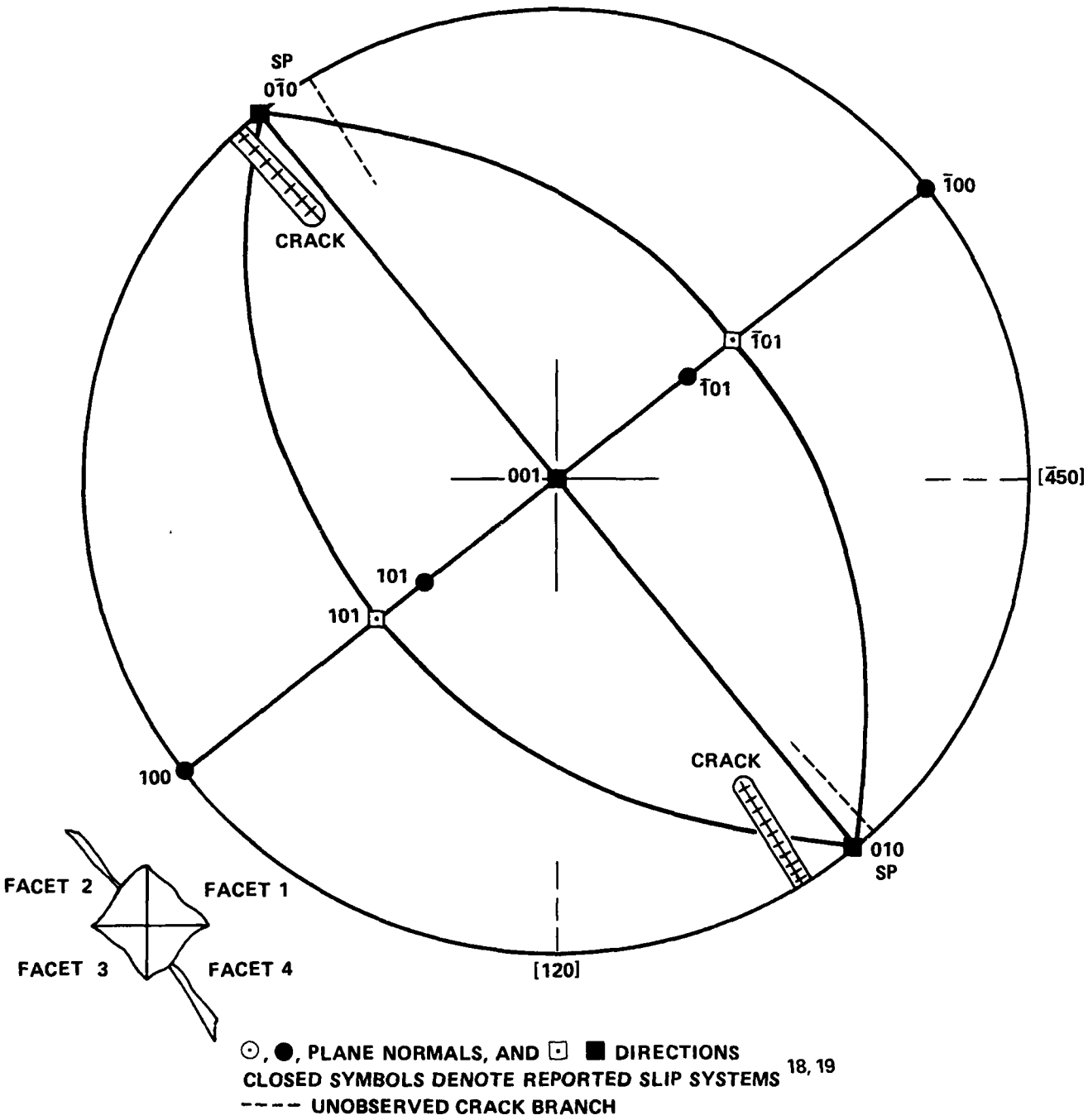

FIGURE 14. STEREOGRAPHIC PROJECTION SHOWING DEFORMATION SYSTEMS FOR DIAMOND PYRAMID (VICKERS) HARDNESS IMPRESSION IN (001) SURFACE OF AMMONIUM PERCHLORATE

in Figures 9 and 10(B) still occurred for the new indentation. Reaction of dislocations on (101) and ($\bar{1}$01) according to the vector equation

$$\frac{1}{2}\left[101\right]_{(\bar{1}01)} + \frac{1}{2}\left[10\bar{1}\right]_{(101)} \dashrightarrow \left[100\right]_{(100)_C}$$

would give a dislocation crack nucleus of orientation close to that exhibited by the observed cracks.[8,33]

Polarized light microscopy was also performed on diamond pyramid (Vickers) hardness impressions put into a LiF single crystal (supplied by Metlab Corporation) to understand the role that known[33] resultant dislocation arrays have on the observed transmitted light. Micrographs are shown in Figure 15 for a [001] diagonal impression (i.e., the orientation appearing in Figure 11) put into the (100) surface using a load of 9.81 N, resulting in a hardness of 144 kgf/mm^2 (1.41 GPa). In the first case shown (Figure 15(A)), the top cross-polarizer or analyzer was oriented along the [010] direction. The same impression is shown (Figure 15(B)) for the analyzer oriented along the [011] direction. In both instances, the cross-polarizers were rotated to provide maximum extinction. Only a small amount of transmitted light appears to be coming from underneath the four facets of the impression itself. The large amount of transmitted light observed outside of the impression is attributed to the far reaching edge dislocation arrays (Figure 11) aligned in the $\pm$[011] and $\pm$[0$\bar{1}$1] directions. No transmitted light appears to be associated with the screw dislocation arrays[33] aligned in the $\pm$[001] and $\pm$[010] directions. The combined results are in agreement with Mendelson's previously mentioned observation[30] that birefringence in glide bands of NaCl single crystals is due to edge (and not screw) dislocations.

The pattern of transmitted light appearing in Figure 15(A) closely resembles analogous polarized light microscropy results reported by Ahern, Mills, and Westwood[34] for ball impacts on the (001) surface of MgO. The change in the pattern that is observed on comparing Figures 15(A) and 15(B) is attributed to the orientational relation that exists between the polarization vector of the analyzer and the principal (dilatational) stresses, σ_{xx} and σ_{yy}, present for an edge dislocation. In Figure 15(A), both of these principal stresses are contributing a component to the transmitted light. However, no σ_{yy} contribution occurs in Figure 15(B) since the σ_{yy} axis is now orthogonal to the polarization vector of the analzyer.

INITIAL STUDY OF SHOCK REACTIVITY AND DEFORMATION IN AP

Performing shock experiments on relatively small AP samples (~0.5 g) required the development of an experimental technique

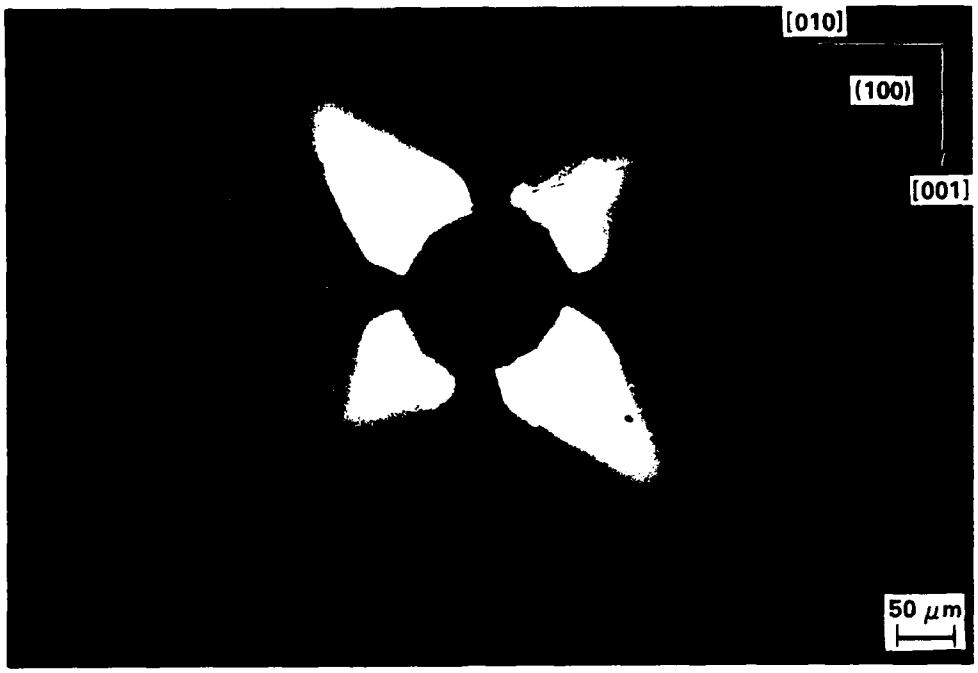

(A) CROSS POLARIZER ORIENTED ALONG [010]

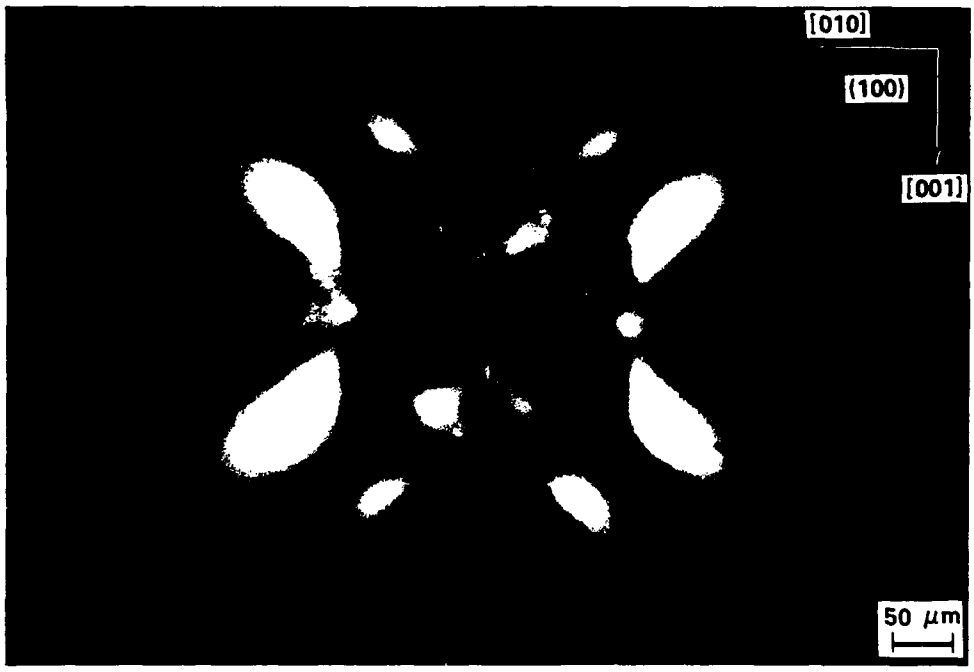

(B) CROSS POLARIZER ORIENTED ALONG [011]

FIGURE 15. DIAMOND PYRAMID (VICKERS) HARDNESS IMPRESSION IN (100) SURFACE OF LITHIUM FLUORIDE VIEWED IN POLARIZED LIGHT WITH CROSS POLARIZER ORIENTED ALONG (A) [010] AND (B) [011]

and the adaptation of instrumentation for dynamic measurements. To date, high-speed photography has been used for dynamic observations, and infrared radiometry is being considered for inclusion in future experiments. Recovered samples have been analyzed by liquid ion chromatography for a very sensitive determination of decomposition. The material properties of recovered samples can be studied by the methods discussed in the last section of the report. The development of the experiments progressed with pellets of pressed AP powder in order to conserve crystals. Readily available 200 μm AP was pressed, for example, into a 12.7 mm diameter by 5.1 mm cylinder at 99.0% TMD with an applied stress of 4.20 kbar. The somewhat translucent pellets had good structural integrity, but the 1% porosity and the pressing process result in AP samples which could be significantly different from the single crystal that was being replicated. All of the reported data were obtained with large (1x1x0.2 cm thick) single AP crystals, also supplied by T. Boggs, NWC.

Two techniques were explored for shocking AP crystals. One approach was projectile impact of a confined sample, similar to earlier work by Macek and Durfee.[24] A Lexan projectile impacted a Lexan sample holder with a 9.5 mm diameter by 6.4 mm long cavity containing the AP. The AP sample consisted of 200 μm crystals pressed to 89 %TMD, much like the samples investigated by Macek and Durfee. At the only projectile velocity attempted, 340 m/s, the sample holder withstood the initial 5.3 kbar shock and subsequent reverberations, as well as the interior pressure generated from any AP decomposition. One problem that would be difficult to resolve with this technique is determining the pressure history of the confined sample. Also, high-speed photography and infrared radiography would require optical fibers to view the sample in its holder. Although this technique is not being actively pursued, it may be suitable for experiments requiring the recovery of well protected samples for microstructural or chemical analyses. An alternative to this technique is the "typical" gas gun experiment, in which the sample is directly impacted. During the first pass of the shock through the sample, optical measurements can be made through the unrestricted rear surface of the sample and the pressure loading can be quantified; however, these are expensive experiments that may be suitable only after some understanding is obtained through other approaches.

The other proposed technique for shocking AP crystals is the one in which the following data were obtained. This approach involves immersing the crystal in a liquid along with an explosive donor at a known separation. In previous work on larger explosive samples, the liquid was most often water, and the experiment was conducted in some sort of aquarium. "Aquarium" testing 1) accommodates the geometric irregularities of cleaved crystals, 2) allows dynamic optical measurements, and 3) permits recovery of shocked crystals. The technique has been

adapted to a bench top experiment by restricting the explosive donor to a detonator. Light mineral oil (baby oil) was the shock transmitting liquid in the experiments for the data reported below; however, other liquids were evaluated. The peak shock pressure in each liquid as a function of distance from the detonator was calculated from streak camera measurements of shock velocity. Also, the shock pulse in water was recorded with a carbon gage. The technique, the various liquids that were considered, and the calibration of shock pressure in those liquids are discussed in Appendix A.

In a series of exploratory experiments, the shock loading on single AP crystals, about 0.2 to 0.4 g each, was varied in order to determine the thresholds for fracture and decomposition. Surviving at least weak shocks is necessary for those crystals to be recovered for microstructural evaluation and/or mechanical testing, such as microindentation hardness testing. When stronger shocks are desired for decomposition studies, the crystal fragments need to be large enough in order to recover them for chemical analysis. Since fragments are satisfactory, this is an improvement over requiring a capsule for the sample that remains sealed throughout the experiment. In the earlier work of Macek and Durfee,[24] the pressed AP powder was encapsulated so that decomposition could be determined by weight loss. Also, encapsulation of the sample complicates the experiment as was previously discussed for the projectile impact technique.

A very sensitive chemical analysis technique, liquid ion chromatography (LIC), was used in the current study. In addition to not requiring all of the original sample, the technique can be used to quantify the decomposition in a local region, such as at a microhardness indentation. For example, an indented crystal could be weakly shocked so that decomposition occurs only in the vicinity of the strain field around the indentation. The bulk of the crystal, which supported the indented region for the purpose of recovery, would be cleaved away prior to analysis with LIC or possibly other techniques. In the reported analyses, about 100 mg of each recovered sample was cleaned in pentane and then dissolved in water for obtaining the concentrations of Cl^-, ClO_3^-, NO_2^-, and NO_3^-. The relative accuracy of those measurements is no greater, and perhaps significantly poorer, than $\pm 10\%$; for ClO_3^- the accuracy may only be $\pm 30\%$. Since exposed surfaces of the samples are cleaned, the technique should record decomposition interior to those boundaries and be unaffected by surface contamination or reaction. Complete details of the LIC analysis scheme developed for this study are described in Appendix B.

The five exploratory experiments are summarized in Table 1. The crystal in each case was resting on a piece of oil soaked polyurethane foam (Figure A-2) or supported above a piece of foam by a 0.05 mm thickness of tape, so that the camera view of the crystal was unobstructed. These arrangements minimized any impedance mismatch between the oil and the supports, while

providing a good catcher for the crystal. Except for the weakest shock loadings, the crystal or its fragments were found buried in the foam. Although, those crystals recovered intact experienced the weaker shocks, the pressures are still supposed to be quite high relative to the yield stress.

TABLE 1. OBSERVATIONS AND CHEMICAL ANALYSES OF AP CRYSTALS SHOCKED IN LIGHT MINERAL OIL

Gap (mm)	Pressure in Oil (kbar)	Observations	Chemical Analysis (ppm) Cl^-	NO_2^-	NO_3^-	ClO_3^-
Not shocked, microhardness indentation			420	8	46	4
35	0.6	No damage	600	8	29	25
23	1.3	No damage	530	12	38	22
15	2.8	No damage	410	18	39	10
8.2	8.7	Broke into five pieces	520	20	45	20
5.0	24	Large pieces were 88% of original weight	11,000	8	46	4

The shot with the shortest gap listed in Table 1 was filmed at a rate of two million frames per second with an Imacon electronic camera. The photographs in Figure 16 show that the shock was still quite curved when entering the crystal and that the gas bubble from the expanding detonation products, which are opaque to the backlighting, reached the crystal shortly after the shock. The shock curvature and the additional gas bubble loading both should have contributed to the breakup of the crystal. The same setup, without a crystal, was filmed at a rate one million frames per second with the same camera. The sequence of photographs in Figure 17 show that the gas bubble expands slowly after the first 5 μs; therefore, direct interaction of the crystal with the gas bubble was probably not a factor in the other shots listed in Table 1 because of the larger gaps. In future tests, a less curved shock with the same peak pressure could be achieved by using a larger explosive donor. This would also alleviate the problem associated with the gas bubble impinging upon the crystal. The larger donor would require, at least for safety reasons, moving the experimental apparatus into the firing chamber.

There appears to be little change in the ion concentrations listed in Table 1 except for the shot with the shortest gap. In that test, there was a tremendous increase in the Cl^- concentration while the other ion concentrations remained relatively unchanged. It was surprising that Cl^- was so high and

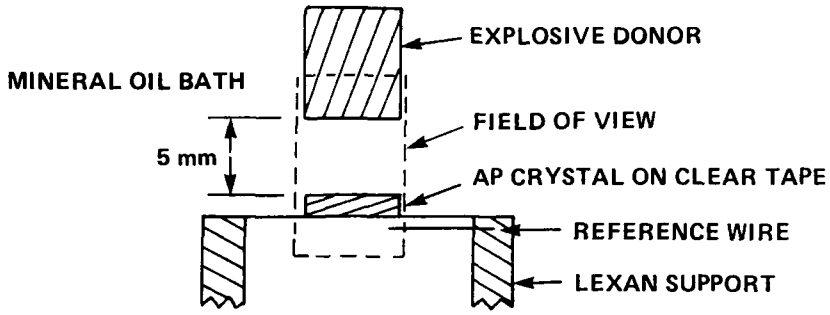

RELATIVE TIME FOR EACH FRAME LISTED IN MICROSECONDS

THIS CRYSTAL WAS RECOVERED AND ANALYZED BY ION CHROMATOGRAPHY FOR REACTION PRODUCTS.

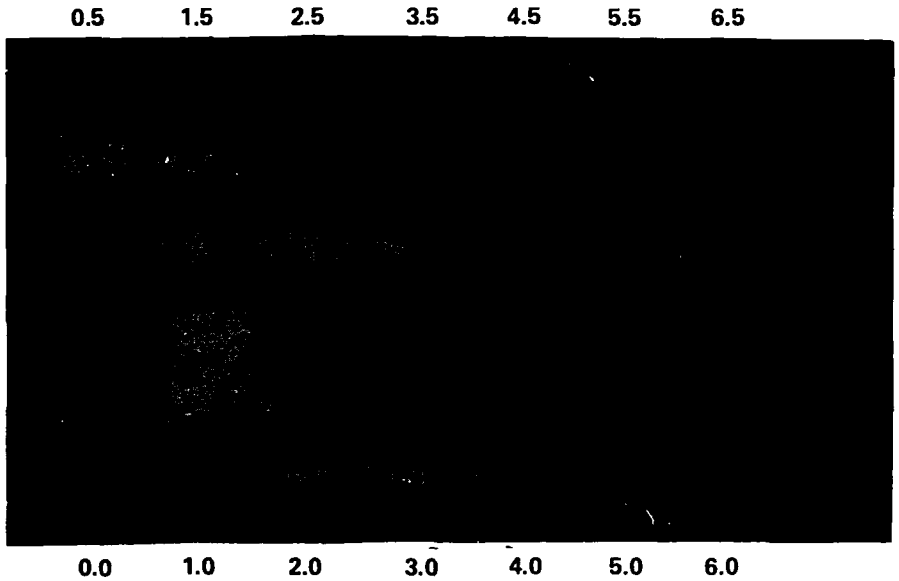

DESCRIPTION OF EVENTS SEEN IN INDIVIDUAL FRAMES

0.0 μs NO ACTION
0.5 μs LUMINOUS DETONATION WAVE PROPAGATING IN EXPLOSIVE
1.0 μs LUMINOUS DETONATION WAVE AT END OF EXPLOSIVE DONOR
1.5 μs EXPLOSIVELY DRIVEN SHOCK JUST ENTERING MINERAL OIL
2.0 μs SHOCK WAVE APPROACHING CRYSTAL; LUMINOUS DETONATION PRODUCTS SEEN JUST BEHIND SHOCK WAVE
2.5 μs SHOCK WAVE ENTERING AP CRYSTAL; SMALL ZONE OF WEAK LUMINOSITY AT CRYSTAL/OIL INTERFACE
3.0 μs SHOCK WAVE JUST COMPLETED PASSAGE THROUGH CRYSTAL; DETONATION PRODUCTS NOW IMPINGING ON UPPER SURFACE

SUBSEQUENT FRAMES MOSTLY OBSCURED BY DETONATION PRODUCT GASES

FIGURE 16. BACKLIT FRAMING CAMERA RECORD OF AN AMMONIUM PERCHLORATE CRYSTAL IN MINERAL OIL BEING SHOCK LOADED

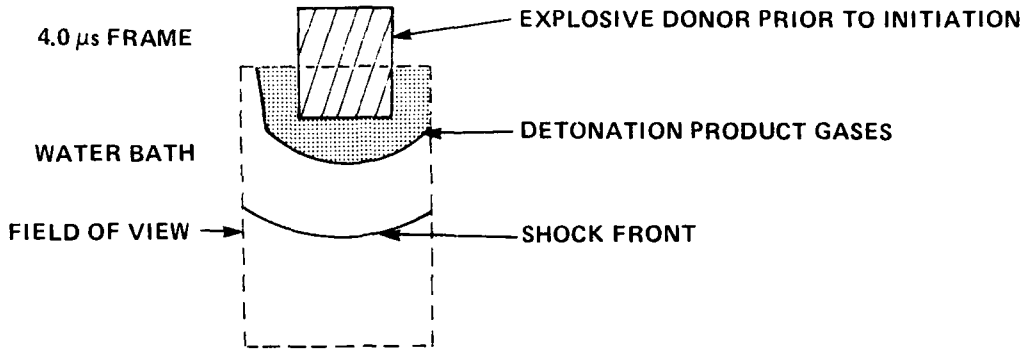

RELATIVE TIME FOR EACH FRAME LISTED IN MICROSECONDS

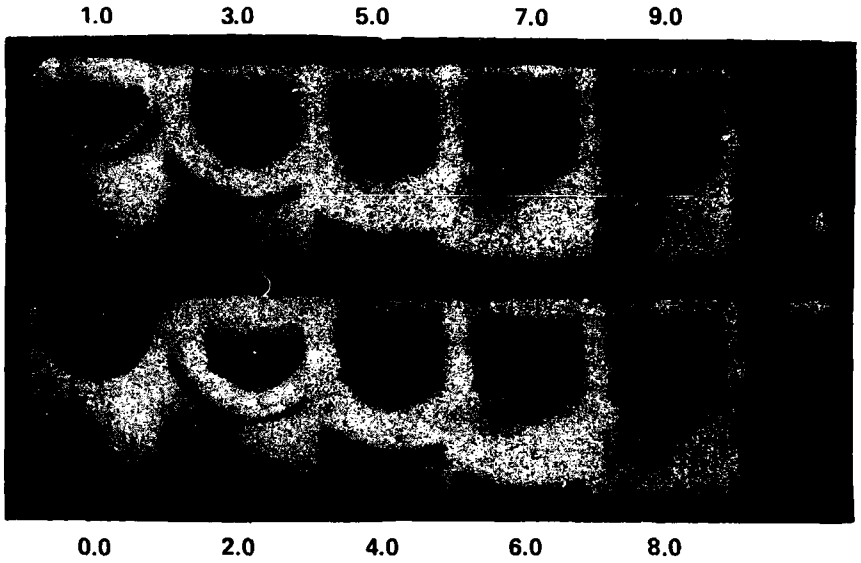

DESCRIPTION OF EVENTS SEEN IN INDIVIDUAL FRAMES

0.0μs SHOCK WAVE HAS JUST EMERGED FROM DETONATOR
1.0-5.0μs SHOCK FRONT PROPAGATES FROM 5.6 mm to 13.2 mm FROM DETONATOR
6.0μs SHOCK FRONT AT EDGE OF FIELD OF VIEW

SUBSEQUENT FRAMES SHOW LITTLE EXPANSION OF THE DETONATION PRODUCT GASES

FIGURE 17. BACKLIT FRAMING CAMERA RECORD OF THE SHOCK FRONT AND GAS BUBBLE FROM A DETONATOR INITIATED IN WATER

yet NO_2^- and NO_3^- remained about the same as for the other shots. Assuming there was no gross contamination, the oxidized form of nitrogen, relative to AP, might not be nitrite or nitrate, but instead neutral gaseous species: N_2, NO, N_2O, and NO_2.[35] These nitrogen species would either escape from the crystal, or, if they were trapped inside, would not be separated by ion chromatography.

The threshold of reaction appears to be between the shots with the 8.2 and 5.0 mm gaps. The shock pressure in oil for these shots was 8.7 and 24 kbar, respectively; the shock pressure in the crystal would be somewhat higher. The threshold for reaction in pressed samples of AP with 13% porosity was about 9 kbar for a shock 12 μs in duration and about 5 kbar for a shock 21 μs in duration.[24] The shock duration in the current aquarium experiments is only approximately 1 μs, and so the threshold of reaction should be greater than 9 kbar. More experiments are required to further define the threshold.

While conducting the previous experiments, a most interesting observation resulted when the detonator failed to function properly because of being oil soaked. The explosion of the detonator bridgewire, by a 5 μf capacitor charged to 2.5 kV, and the probable reaction of only a small amount of explosive drove a series of compressive waves into the mineral oil for approximately 20 μs. The streak camera record of the event is shown in Figure 18. About 11 μs after the first wave interacted with the crystal, the backlighting failed to be transmitted through one zone of the crystal for 3.2 μs. During the 27 μs period of observation following the first wave, two other dark zones occurred, one for 0.7 μs and the other for 6.7 μs. These zones averaged about 0.2 mm in size; if zones at least one order of magnitude smaller had existed they would still be observable on the film. It is postulated that the dark zones in the crystal are associated with slip band formation.

SUMMARY

Work has commenced on investigating the roles that deformation, fracture, and the resultant material microstructure have on the shock reactivity of AP. A cleaved single crystal of AP was oriented by performing a standard zone analysis on a Laue back-reflection photograph. This analysis was accomplished using computer-generated standard projections for AP which involved creating software that was adapted from the work of other researchers. An initial study of the diamond pyramid (Vickers) microindentation hardness was performed for the $(\bar{2}10)$ and (001) cleavage surfaces. The indentation-forming (primary deformation) and volume-accommodating (secondary deformation) slip systems were successfully identified. A number of the slip systems have

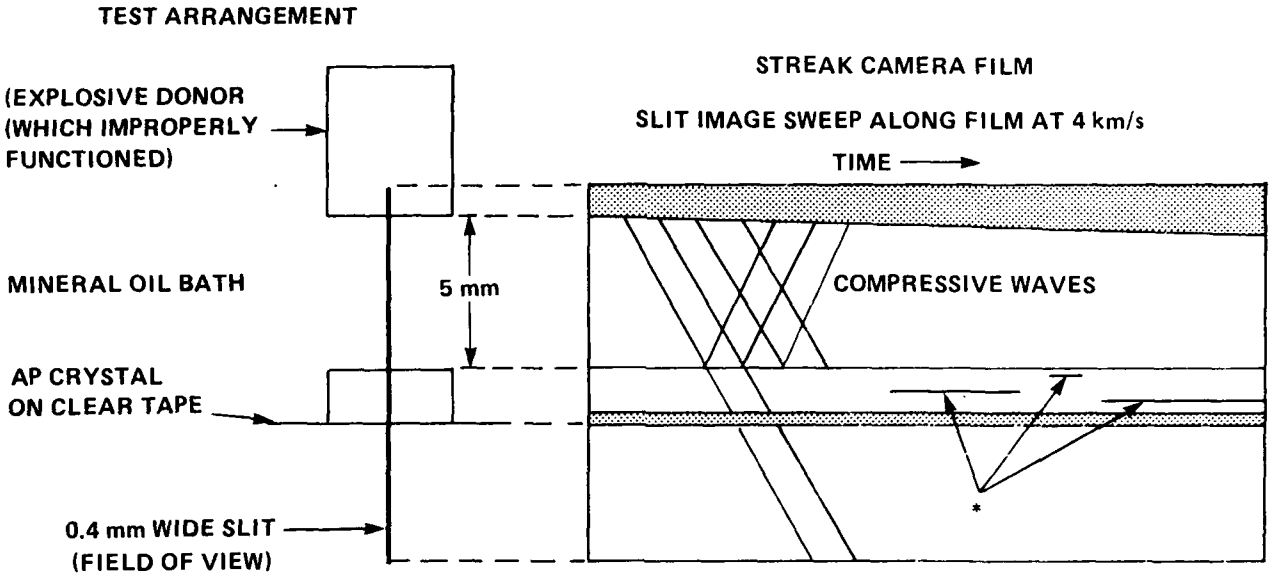

*MOMENTARY DARK ZONES IN CRYSTAL ASSUMED TO BE DUE TO MICROSTRUCTURAL CHANGES

FIGURE 18. BACKLIT STREAK CAMERA RECORD OF AN AMMONIUM PERCHLORATE CRYSTAL IN MINERAL OIL BEING COMPRESSIVELY LOADED

not been previously reported. The easiest operative slip system was found to be (100)[001]. Particularly noteworthy was the observation that cracking occurred in the regions of greatest plastic deformation. Dislocation reactions, involving two dislocations meeting and forming a third dislocation, were specified as being responsible for the cracking. Using polarized light microscopy, it was possible to observe the strain field caused by the edge dislocations surrounding the hardness impressions. A rather far reaching strain field, extending beyond the crack tip, was observed for the impression put into the $(\bar{2}10)$ surface. Consequently, the plastic deformation is not nearly so localized for AP as it was observed previously for RDX.

Centimeter size AP single crystals were shock loaded by a detonator while immersed in light mineral oil. The event has been observed by high speed photography, and the apparatus design permitted recovery of each sample for chemical analysis of decomposition by liquid ion chromatography. A dramatic increase in Cl^- occurred in the experiment having the strongest shock (24 kbar peak pressure in the oil). Weakly shocked samples (peak pressures in the oil up to 3 kbar) were recovered intact, a condition that would make them particularly suitable for subsequent mechanical testing and microstructural characterization. High speed photographs of a backlit crystal that was loaded by a rapid series of compressive waves exhibited momentary dark zones that are believed to occur because of slip band formation.

REFERENCES

1. Bowden, F. P., and Yoffe, A. D., Fast Reactions in Solids, Butterworths Scientific Publications, London, England, 1958.

2. Green, L. G., and James, E., Jr., "Radius of Curvature Effect on Detonation Velocity," in Proceedings of the Fourth Symposium (International) on Detonation, White Oak, Silver Spring, MD, 12-15 Oct 1965, ACR-126, pp. 86-91.

3. Elban, W. L., and Armstrong, R. W., "Microhardness Study of RDX to Assess Localized Deformation and Its Role in Hot Spot Formation," in Proceedings Seventh Symposium (International) on Detonation, 16-19 Jun 1981, NSWC MP 82-334, pp. 976-985.

4. Elban, W. L., Armstrong, R. W., and Hoffsommer, J. C., "X-Ray Orientation and Hardness Experiments on RDX Explosive Crystals," Journal of Materials Science, Vol. 19, No. 2, 1984, pp. 552-566.

5. Elban, W. L., Coffey, C. S., Armstrong, R. W., Yoo, K.-C., and Rosemeier, R. G., Microstructural Origins of Hot Spots in RDX Explosive and Several Reference Inert Materials, NSWC MP 83-116, Mar 1983, Naval Surface Warfare Center, Silver Spring, MD.

6. Elban, W. L., Hoffsommer, J. C., Coffey, C. S., Yoo, K.-C., and Rosemeier, R. G., Microstructural Origins of Hot Spots in RDX Explosive and a Reference Inert Material, NSWC MP 84-200, May 1984, Naval Surface Warfare Center, Silver Spring, MD.

7. Elban, W. L., Hoffsommer, J. C., Glover, D. J., Coffey, C. S., and Armstrong, R. W., Microstructural Origins of Hot Spots in RDX Explosive and Several Reference Inert Materials, NSWC MP 84-358, Nov 1984, Naval Surface Warfare Center, Silver Spring, MD.

8. Armstrong, R. W., and Elban, W. L., "Dislocation Aspects of Plastic Flow and Cracking at Indentations in Magnesium Oxide and Cyclotrimethylenetrinitramine Explosive Crystals," in Microindentation Techniques in Materials Science and Engineering, Eds.: Blau, P. J., and Lawn, B. R., American Society of Testing and Materials, Philadelphia, PA, 1986, ASTM STP 889, pp. 109-126.

REFERENCES (Cont.)

9. Westbrook, J. H., and Conrad, H., Eds., The Science of Hardness Testing and Its Research Applications, American Society for Metals, Metals Park, OH, 1973.

10. Blau, P. J., and Lawn, B. R., Eds., Microindentation Techniques in Materials Science and Engineering, American Society of Testing and Materials, Philadelphia, PA, 1986, ASTM STP 889.

11. Heavens, S. N., and Field, J. E., "The Ignition of a Thin Layer of Explosive by Impact," Proceedings of the Royal Society of London, Ser. A, Vol. 338, No. 1612, pp. 77-93.

12. Connick, W., and May, F. G. J., "Dislocation Etching of Cyclotrimethylene Trinitramine Crystals," Journal of Crystal Growth, Vol. 5, No. 1, 1969, pp. 65-69.

13. Tanner, B. K., X-Ray Diffraction Topography, Pergamon Press, Oxford, England, 1976.

14. Armstrong, R. W., "Laboratory Techniques for X-Ray Reflection Topography," in Characterization of Crystal Growth Defects by X-Ray Methods, Eds.: Tanner, B. K., and Bowen, D. K., Plenum Press, New York, NY, 1980, pp. 349-367.

15. Hoffsommer, J. C., Glover, D. J., and Elban, W. L., "Quantitative Evidence for Nitroso Compound Formation in Drop-Weight Impacted RDX Crystals," Journal of Energetic Materials, Vol. 3, No. 2, 1985, pp. 149-167.

16. Hoffsommer, J. C., and Glover, D. J., "Thermal Decomposition of 1,3,5-Trinitro-1,3,5-Triazacyclohexane (RDX): Kinetics of Nitroso Intermediates Formation," Combustion and Flame, Vol. 59, No. 3, 1985, pp. 303-310.

17. Coffey, C. S., and Jacobs, S. J., "Detection of Local Heating in Impact or Shock Experiments with Thermally Sensitive Films," Journal of Applied Physics, Vol. 52, No. 11, 1981, pp. 6991-6993.

18. Herley, P. J., Jacobs, P. W. M., and Levy, P. W., "Dislocations in Ammonium Perchlorate," Journal of the Chemical Society, Section A, No. 3, 1971, pp. 434-440.

19. Williams, J. O., Thomas, J. M., Savintsev, Y. P., and Boldyrev, V. V., "Dislocations in Orthorhombic Ammonium Perchlorate," Journal of the Chemical Society, Section A, No. 11, 1971, pp. 1757-1760.

REFERENCES (Cont.)

20. Price, D., Clairmont, A. R.,Jr., Erkman, J. O., and Edwards, D. J., "Infinite Diameter Detonation Velocities of Ammonium Perchlorate," Combustion and Flame, Vol. 13, No. 1, 1969, pp. 104-108.

21. Price, D., Clairmont, A. R.,Jr., and Erkman, J. O., The NOL Large Scale Gap Test. III. Compilation of Unclassified Data and Supplementary Information for Interpretation of Results, NOLTR 74-40, 8 Mar 1974, Naval Surface Warfare Center, Silver Spring, MD.

22. Dick, J., "Plane Shock Initiation of Detonation in γ-Irradiated Pentaerythritol Tetranitrate," Journal of Applied Physics, Vol. 53, No. 9, 1982, pp. 6161-6167.

23. Dick, J., "Effect of Crystal Orientation on Shock Initiation Sensitivity of Pentaerythritol Tetranitrate Explosive," Applied Physics Letters, Vol. 44, No. 9, 1984, pp. 859-861.

24. Macek, A., and Durfee, R. L., A Study of Energy Release in Rocket Propellants by a Projectile Impact Method, NASA Contractor Report No. 66395, 9 Jun 1967, Atlantic Research Corporation, Alexandria, VA.

25. Kosel, T. H., "Computational Techniques for Stereographic Projection," Journal of Materials Science, Vol 19, No. 12, 1984, pp. 4106-4118.

26. Kosel, T. H., "Microcomputer Stereographic Projection," Journal of Metals, Vol. 37, No. 10, 1985, pp. 56-57.

27. Staley, J. T., "PC Programs for Materials Science - Part II," Journal of Metals, Vol. 37, No. 3, 1985, p. 71.

28. Staley, J. T., "PC Programs for Materials Science - Part III," Journal of Metals, Vol. 37, No. 4, 1985, p. 76.

29. Swanson, H. E., Gilfrich, N. T., and Cook, M. I., Standard X-Ray Diffraction Powder Patterns, National Bureau of Standards Circular 539, Vol. 7, 27 Sep 1957, p. 6.

30. Mendelson, S., "Birefringence Due to Dislocations in Glide Bands of Rocksalt Single Crystals," Journal of Applied Physics, Vol. 32, No. 10, 1961, pp. 1999-2004.

31. Elban, W. L., Armstrong, R. W., Yoo, K. C., Rosemeier, R. G., and Yee, R. Y., "X-Ray Reflection Topographic Study of Growth Defect and Microindentation Strain Fields in an RDX Explosive Crystal," to be published in the Journal of Materials Science.

REFERENCES (Cont.)

32. Yoo, K.-C., Rosemeier, R. G., Elban, W. L., and Armstrong, R. W., "X-Ray Topography Evidence for Energy Dissipation at Indentation Cracks in MgO Crystals," Journal of Materials Science Letters, Vol. 3, No. 6, 1984, pp. 560-562.

33. Armstrong, R. W., and Wu, C. Cm., "Lattice Misorientation and Displaced Volume for Microhardness Indentations in MgO Crystals," Journal of the American Ceramic Society, Vol. 61, Nos. 3-4, 1978, pp. 102-106.

34. Ahern, J.S., Mills, J.J., and Westwood, A.R.C., "Short-Time Chemomechanical Effects in MgO," Journal of Applied Physics, Vol. 50, No. 5, 1979, pp. 3699-3701.

35. Whitehead, H.M., and Jacobs, P.W.M., "Decomposition and Combustion of Ammonium Perchlorate," Chemical Reviews, Vol. 69, No. 4, 1969, pp. 551-590.

PRESENTATIONS AND PUBLICATIONS

1. "Deformation Studies on Ammonium Perchlorate Relating to Shock Initiated Reaction," W.L. Elban, ONR Workshop on Dynamic Deformation, Fracture, and Transient Combustion, Chestertown, MD, 12-14 May 1987, CPIA Publication 474, 1987, pp. 35-45.

2. "Shock Initiated Reaction in Deformed Crystals of Ammonium Perchorate," H.W. Sandusky, R.R. Bernecker, B.C. Glancy, and D. Carlson, ONR Workshop on Dynamic Deformation, Fracture, and Transient Combustion, Chestertown, MD, 12-14 May 1987, CPIA Publication 474, 1987, pp. 47-54.

APPENDIX A

AQUARIUM TESTING

An aquarium technique was recently implemented for shock initiation studies at NSWC.[A-1] In that arrangement, the explosive donor from the NOL Large Scale Gap Test (LSGT)[A-2] is separated from the test sample by a gap chosen to achieve the prescribed pressure in the sample; the entire arrangement is immersed in water. The calibration of the shock pressure in water versus distance from the LSGT donor (porous pentolite, 50.8 mm diameter by 50.8 mm high) was calculated[A-3] and determined experimentally;[A-1] other donor configurations were also studied.[A-3,A-4]

The aquarium technique was suitable for shock reactivity studies of AP crystals since it accommodates the geometric irregularities of cleaved crystals and readily permits dynamic optical measurements. A small donor in comparison to the above gap tests was desired for several reasons: (1) the crystals are relatively small (largest dimension being less than 10 mm); (2) high amplitude shocks (>20 kbar) should not be necessary to examine the onset of reaction or microstructural changes in the material; and (3) a smaller donor increases the possibility of recovering a sample for chemical analysis or assessment of microstructural changes. Also, a small donor permitted the development of a containment vessel for safely conducting bench top experiments in the laboratory. The laboratory environment simplifies the experiment and its instrumentation, especially close-up photography with high-speed cameras. The donor is a Reynolds RP-80 exploding bridgewire detonator, which contains 217 mg of explosive. As will be shown, the shock pulse is short (approximately 1 μs) and declines very rapidly near the donor, attenuating to about 20 kbar at a 5 mm separation.

Several liquids have been used in the testing: water, mineral oil (both heavy and light grades) and cyclohexane. All are transparent for high-speed photography and the shock properties (Hugoniots) have been determined by other investigators. Information about the liquids are summarized in Table A-1. The shock Hugoniot for water has been studied over a wide pressure range and is well established;[A-5,A-6] however, AP quickly dissolves in water. Even so, an AP sample was sealed

TABLE A-1. LIQUIDS FOR AQUARIUM EXPERIMENTS

Liquid	Source	ρ (g/cc)	c_o (mm/μs)	Hugoniot U (mm/μs)	Flash Point (°C)
Water	Distilled	0.998	1.483	c_o+10.990ln(1+u/5.19)	
Mineral Oil (Paraffin Oil)					229
Heavy, white	Reagent grade	0.875-0.905 0.87 used*	1.45	2.18+1.53u, p>15kbar 1.45+2.71u, p<15kbar	
Light	Giant Food baby oil with fragrance	0.83-0.86	1.40	Assumed same as above for the heavy oil	
Cyclohexane	Reagent grade	0.776	1.26	1.418+1796u, p<75kbar	-16

Nomenclature and note:
ρ = density
c_o = sound velocity
U = shock velocity
u = particle velocity
* Compatible density with Hugoniot in Reference A-9.

with grease for an initial experiment, and several water experiments were useful in developing instrumentation. Both mineral oil and cyclohexane do not dissolve AP and are not likely to decompose (Reference A-7 concerning cyclohexane) or react with the AP during the shocking process. The advantages of cyclohexane are that: (1)it is a single chemical entity instead of a blend of paraffins; (2) the Hugoniot can be better established below 15 kbar, as discussed below; and (3) it is easier to clean up. A potential safety problem is that the flash point[A-8] for cyclohexane is only -16°C versus 229°C for mineral oil. Even though the vapors above the cyclohexane were not ignited by the detonator in the one calibration test (Shot ONR-11), it was decided to restrict cyclohexane tests to the firing chamber.

Mineral oil appears safe for laboratory experiments, and a Standard Operating Procedure (SOP #266) was approved for using this liquid in testing outside of the firing chamber. For a 6 mm deep pool of mineral oil, direct impingement with a butane torch for four minutes was required to ignite it, and then the flame extinguished upon removal of the torch. The shock properties are reported[A-9] for the heavy grade. This material was not delivered in time for the initial experiments, so baby oil, a light mineral oil, was purchased locally. The shock properties of the light grade were assumed to be the same as that for the heavy grade.

The reported Hugoniots (i.e., variation of shock velocity with particle velocity) for both mineral oil and cyclohexane have not been established for shock pressures less than 15 kbar nor do they properly extrapolate to zero pressure. This is the case for most liquids except mercury and water, whose shock velocity from the Hugoniot approaches the sound velocity as pressure go to zero. For heavy mineral oil, the variation of shock velocity with particle velocity was linear over the examined range of 15 to 150 kbar.[A-9] The sound velocity for both light and heavy mineral oil was measured to be 1.40 and 1.45 mm/μs, respectively; a measurement of 1.485 mm/μs for water versus the value of 1.483 in Reference A-5 verified the technique. From the sound velocity at zero pressure and the reported shock and particle velocities at 15 kbar, an assumed Hugoniot for heavy mineral oil was generated over the 0 to 15 kbar range. For cyclohexane, the low pressure range (15 to 75 kbar) of the reported Hugoniot[A-10] and the sound velocity can be reasonably fitted, as shown in Figure A-1, using the method of least squares.

The aquarium used in early experiments was a one liter box of clear plastic with an open top. This aquarium was suitable for photography but did not contain the liquid (making for difficult cleanup of mineral oil) or sample after the detonator was initiated. The simple 0.9 liter, closed vessel shown in Figure A-2 was developed for confining these experiments when conducted in either the firing chamber or the laboratory. The shocked AP crystal is driven into a small block of open cell polyurethane foam just under the crystal, both protecting the

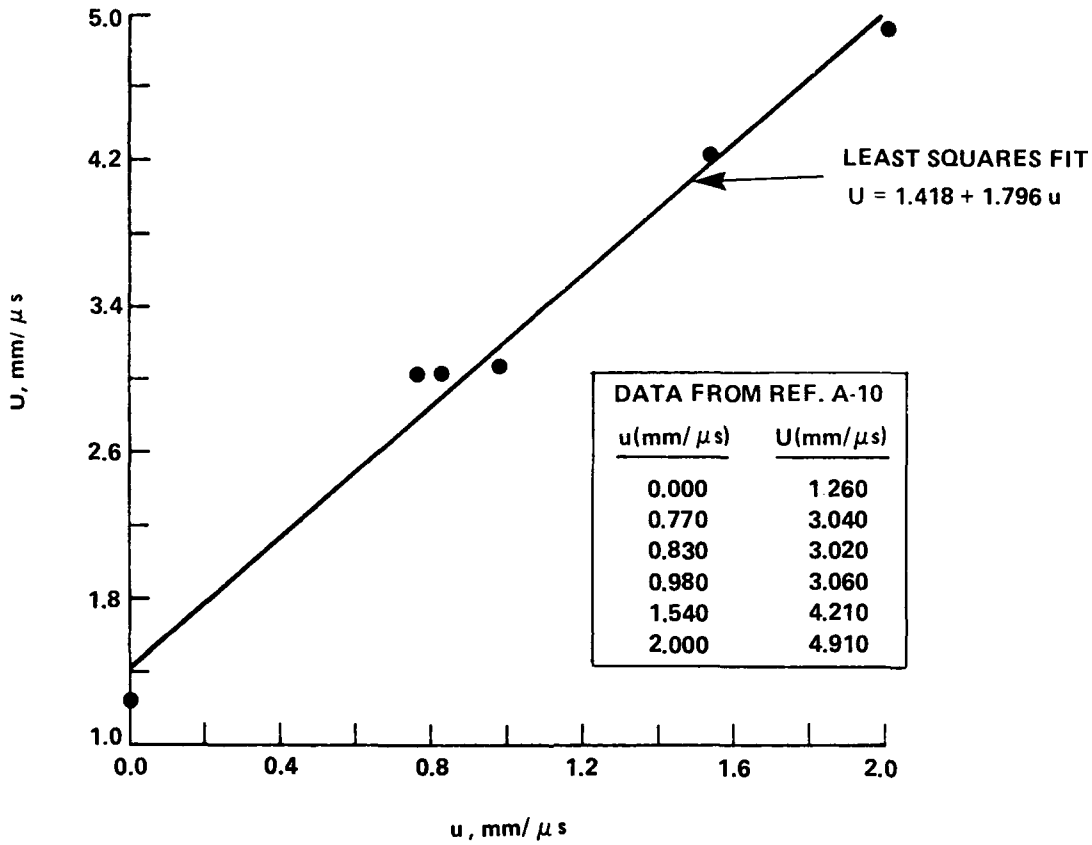

FIGURE A-1. CYCLOHEXANE HUGONIOT FOR PRESSURES LESS THAN 75 kbar

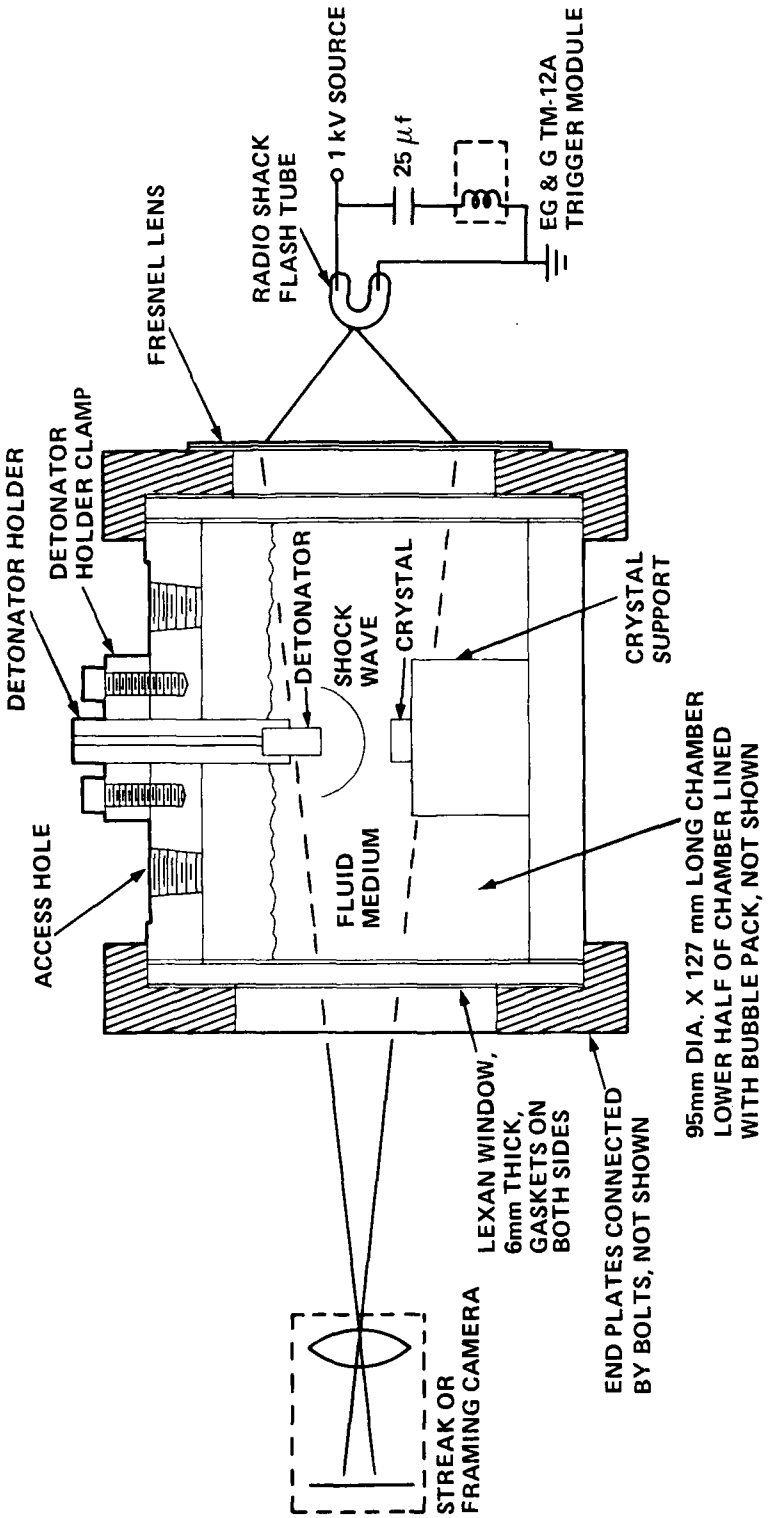

FIGURE A-2. CLOSED CHAMBER FOR PHOTOGRAPHY OF SHOCK REACTION IN SMALL SAMPLES

crystal from subsequent damage and making recovery easy. "Bubble pack" is used along the bottom half of the chamber to attenuate the shock wave prior to reflection from the wall. The use of RP-80 detonators with a Delrin versus a brass sleeve greatly reduces the pitting of the Lexan windows by fragments from the detonator. The closed vessel was used in all of the shock calibration experiments in the discussion that follows.

The procedure for measuring the change in shock pressure as a function of distance from the detonator is essentially the same as that developed, but undocumented, for the larger aquarium tests.[A-1] At and near the shock front in a transparent material, the index of refraction changes; therefore, a backlit view of the medium appears to extinguish as the shock front propagates through it. In the early development of the aquarium technique at NSWC, the backlighting source was a linear xenon flash lamp on the back of the aquarium in line with a projection of the streak camera slit. This diffuse source provided a slight change in film exposure at the shock front; light from various positions along the lamp could be reflected off the curved shock and into the camera. In all subsequent testing, a near-collimated backlighting source provided good definition of the shock front. In this approach, a Fresnel lens on the back of the aquarium focused a small light source onto the center of the objective lens of the camera. The source was a Radio Shack xenon flash tube (catalog number 272-1145) powered by the 1 kV discharge of generally a 25 μf capacitor. In order to obtain as precise a data set as possible, a streak camera (Cordin model 136A) was used with its 60 mm slit image totally devoted to the area of interest.

Film records from aquarium testing provide distance-time data which are differentiated to obtain shock velocity as a function of distance, x, from the donor. Each film record is first digitized with a Micro-Vu Corp. Model V1000 Optical Inspection Instrument that has 2.5 μm resolution and inaccuracies not exceeding 0.1%. Each digitized point, except at the ends of the record, is fit by a quadratic function through itself and the nearest five points on both sides of it. The spacing of the digital data and their accuracy determine the number of points fitted in order to filter out irregularities without altering the character of the data; digitized traces contained 80 to 150 points. The differential of the quadratic function at the central point provided the shock velocity, U, there, which in conjunction with the Hugoniot, defines the particle velocity, u, and pressure ($p = \rho_0 Uu$, where ρ_0 = density). Since pressure is a very sensitive function of shock velocity, errors must be closely controlled. Those errors are estimated to be less than 5%, assuming a correct Hugoniot.

Digitized distance-time traces of the shock fronts are shown in Figure A-3 for the liquids listed in Table A-1. The shock propagates in water and cyclohexane at about the same rate,

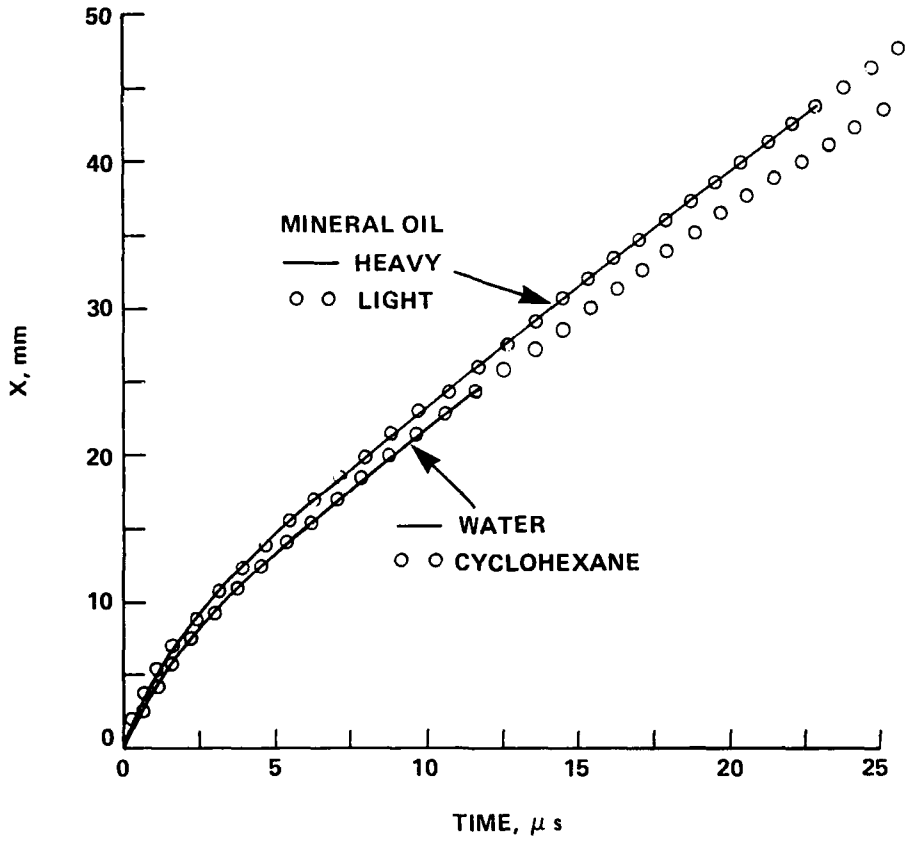

FIGURE A-3. PROPAGATION OF A SHOCK IN VARIOUS LIQUIDS FROM AN RP-80 DETONATOR

slightly faster in mineral oil; differences between light and heavy mineral oil are within experimental error. The calculated pressure-distance (p-x) curves from the above data shown in Figure A-4 for water and cyclohexane are quite similar below 25 kbar. Using the modified Hugoniot shown in Table A-1 for mineral oil, its p-x profile essentially matched that for water. Despite the limitations of the Hugoniots of cyclohexane and especially mineral oil at p less than 15 kbar, shock pressure appears to be relatively independent of the liquid. It was recently recognized, as shown in Figure 2 of Reference A-1, that the p-x profiles from the NOL LSGT donor in water and polymethylmethacrylate (the Plexiglass gap for the LSGT) are approximately the same.

Improving the shock calibrations for cyclohexane and mineral oil are not necessary since the AP Hugoniot must be estimated. Both the p-x data for the liquid and the AP Hugoniot are required in order to calculate the shock pressure that is transferred from the liquid into the AP crystal. In order to verify the calculations that will be made, an independent measurement of pressure with a carbon gage was attempted in two experiments. The Dynasen Model C300-5-EKRTE gage was placed on the back of a 0.05 mm thickness of tape that suspended it in the water 20 mm from the detonator. The outputs were questionable because of a decaying burst of electrical noise from the high voltage pulse which initiates the detonator, requiring that the technique be improved. However, the one gage output with a relatively stable baseline indicated a peak pressure of 1.25 kbar compared with 1.9 kbar from the camera data; the duration of the shock pulse was 1.3 μs. The peak pressure occurred 0.3 μs past the leading edge of the pulse, possibly because of reverberations in the tape and gage package. When a peak is estimated by drawing extrapolated lines through the rise and decay portions of the shock pulse, a 1.9 kbar pressure is obtained. Thus, interpretation may be required for measurements from even a thin gage. The gage certainly provides more than just the peak measurement from camera data; and the gage will be useful for measuring the pressures associated with a series of compressive waves, something which can not be accomplished with a camera.

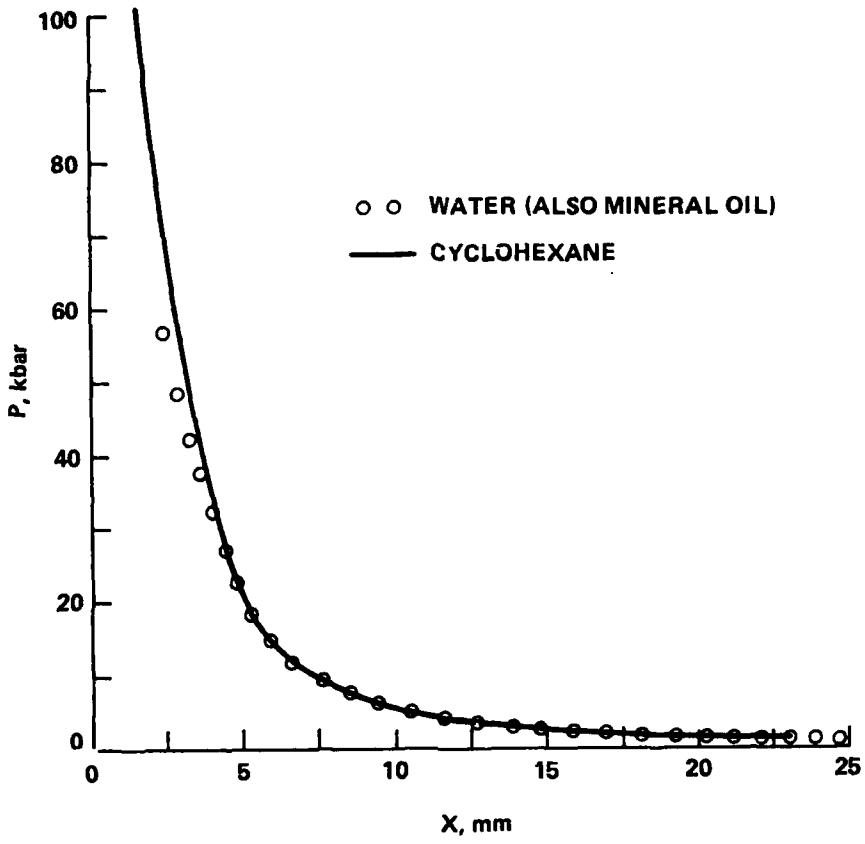

FIGURE A-4. SHOCK PRESSURE IN VARIOUS LIQUIDS AS A FUNCTION OF DISTANCE FROM AN RP-80 DETONATOR

REFERENCES

A-1. Bernecker, R. R., Clairmont, A. R., Jr., Sandusky, H. W., and Smith, M. S., "Participation of Aluminum in Two-Dimensional Shock Initiation Experiments," in Shock Waves in Condensed Matter 1987, Elsevier Science Publishers, New York, NY, 1988, pp. 573-576.

A-2. Price, D., Clairmont, A. R., Jr., and Erkman, J. O., The NOL Large Scale Gap Test. III. Compilation of Unclassified Data and Supplementary Information for Interpretation of Results, NOLTR 74-40, 8 Mar 1974, Naval Surface Warfare Center, Silver Spring, MD.

A-3. Jacobs, S. J., Sternberg, H., and Hudson, L., "Numerical Simulation of Donors for Gap Experiments," in Proceedings of 1988 JANNAF Propulsion Systems Hazards Subcommittee (PSHS) Meeting, to be published.

A-4. Bernecker, R. R. and Clairmont, A. R., Jr., "Shock Sensitivity Test, Insensitive Munitions, and Underwater Explosives," in Proceedings of 1988 JANNAF PSHS Meeting, to be published.

A-5. Rice, M. H. and Walsh, J. M., "Equation of State of Water to 250 Kilobars," The Journal of Chemical Physics, Vol. 26, No. 4, 1957, pp. 824-830.

A-6. Liddiard, T. P. and Forbes, J. W., Shockwaves in Fresh Water Generated by the Detonation of Pentolite Spheres, NSWC TR 82-488, 26 May 1983, Naval Surface Warfare Center, Silver Spring, MD.

A-7. Hayes, B., "Dielectric and State Behavior of Cyclohexane Under Shock Loading," Review of Scientific Instruments, Vol. 46, No. 12, 1975, pp. 1676-1684.

A-8. Sax, N. I., Ed., Dangerous Properties of Industrial Materials, Van Nostrand Reinhold Co., New York, NY, 1975.

A-9. Netherwood, P. and Tauber, D., The Shock Hugoniot of Mineral Oil, BRL MR 2214, Aug 1974, Ballistic Research Laboratories, Aberdeen, MD.

REFERENCES (Cont.)

A-10. Marsh, S. P., Ed., LASL Shock Hugoniot Data, University of California Press, Berkeley, CA, 1980.

APPENDIX B

CHEMICAL ANALYSIS OF AMMONIUM PERCHLORATE CRYSTALS

Instrument:	Dionex 2020i Ion Chromatograph
Columns:	Dionex HPIC-AG1 Guard Column (monoanion separation) Dionex HPIC-AS1 Column (monoanion separation) Dionex Anion Fiber Suppressor
Mobile Phase:	2.3 ml/min carbonate buffer (0.0030 M $NaHCO_3$, 0.0024 M Na_2CO_3) Suppressor eluent (0.025 N H_2SO_4)
Injection Volume:	50 μl
Detectors:	Built in Dionex conductivity detector with a sensitivity of 0.3-1 mcs full scale HP 1083A variable wavelength UV detector operating at 206 nm, sensitivity of 0.1 AUFS
Standards:	Anion standard is approximately 10^{-6} M Cl^-, $2x10^{-6}$ M NO_2^-, and $5x10^{-6}$ M NO_3^- Chlorate standard is approximately $5x10^{-6}$ M ClO_3^-, made same day as analysis
Unknown:	0.1 M AP solution in water; 1/10 or 1/100 dilutions of 0.1 M solution as needed

The two standards were run several times to obtain average response factors (based on peak height) for the anions. Response factors were obtained with the conductivity detector for chloride, nitrate, and chlorate ions, and with the UV detector for nitrite and nitrate ions. Typical retention times (which vary from column to column) are: Cl^-, 4.4 minutes; NO_2^-, 6.1 minutes; NO_3^- and ClO_3^- (which co-elute), 19 minutes.

The unknowns are analyzed in the following order: first the 0.001 M AP solution (if used), then the 0.01 M AP solution (if used), and finally the 0.1 M AP solution. This order is necessary because the AP, especially at the higher concentrations, disrupts column function in the following ways: (1) very noisy detector signals immediately after injection, (2) significant shortening of peak retention times, and (3) eventual appearance of a huge background trace which renders the column

unusable until cleaned. Normally, after running the 0.1 M AP solution, the column must be removed and cleaned. This is done by running through the column at 2.0 ml/min the following solutions: (1) 30 ml or more of distilled water, (2) 30 ml or more of 0.1 M Na_2SO_4, (3) 30 ml or more of 0.1 M Na_2CO_3, and (4) 120 ml or more of anion eluent. Cleaning is performed on another liquid chromatography pump. During cleaning, the column eluent goes directly to waste and is not sent through the detectors.

Data reduction is performed using the following procedure. Chloride is determined from one of the runs involving a diluted AP solution (0.01 or 0.001 M). Not only is there usually a larger amount of Cl^- present in the sample, but the disruption of the column by the 0.1 M AP solution immediately after injection can interfere with Cl^- detection since it is the first anion to emerge. Values reported for Cl^- are based on the relative peak heights from the unknown and anion standard. Nitrite, nitrate, and chlorate are determined from the run with the 0.1 M AP solution. Nitrite and nitrate are quantified using the relative peak heights of the unknown and standard from the UV detector. The coincident elution of NO_3^- and ClO_3^- is not a problem since ClO_3^- is transparent to UV. Once NO_3^- is determined by UV, the expected conductivity peak for the AP unknown is calculated. The observed conductivity peak is generally higher, and the difference is attributed to the presence of ClO_3^-. This difference, relative to the peak height for the ClO_3^- standard, provides the chlorate concentration in the unknown. Because the chlorate is not separately detected in the unknown, the error in the reported values may be as high as $\pm 30\%$. The accuracy for the other ions is no greater, and perhaps significantly poorer, than $\pm 10\%$.

DISTRIBUTION

	Copies
Office of Naval Technology Attn: ONT-20T (Dr. L.V. Schmidt) Arlington, VA 22217	1
Commandant of the Marine Corps. Attn: Code RD-1 (Dr. A.L. Slafkosky) Scientific Advisor Washington, DC 20380	1
Office of Naval Research Attn: Code 1132P (Dr. R.S. Miller) Arlington, VA 22217	10
AFATL - DLJG Attn: Mr. O.K. Heiney Elgin AFB, FL 32542	1
AFRPL Attn: DY/MS-24 (Mr. R. Geisler) Edwards AFB, CA 93523	1
Air Force Office of Scientific Research Directorate of Aerospace Science Bolling Air Force Base Washington, DC 20332	1
Air Force Office of Scientific Research Attn: Dr. D.L. Ball Directorate of Chemical and Atmospheric Sciences Bolling Air Force Base Washington, DC 20332	1
NJSRL/NC Attn: Dr.J.S. Wilkes,Jr. USAF Academy, CO 80840	1
Aerojet Strategic Propulsion Co. Attn: Dr. R.L. Lou Bldg. 05025 - Dept. 5400 MS 167 P.O. Box 15699C Sacramento, CA 95813	1
Commander U.S. Army Missile Command Attn: DRSMI-RKL (Dr. W.W. Wharton) Redstone Arsenal, AL 35898	1
Chemical Systems Division Attn: Dr. C.M. Frey P.O. Box 358 Sunnyvale, CA 94086	1
Library of Congress Attn: Gift and Exchange Division Washington, DC 20540	4

DISTRIBUTION (Cont.)

	Copies
Defense Technical Information Center DTIC-DDA-2 Cameron Station Alexandria, VA 22314	12
Lawrence Livermore Laboratory University of California Attn: Code L-324 (Dr. R. McGuire) Livermore, CA 94550	1
Naval Weapons Center Attn: NEDED Yorktown, VA 23691	1
Naval Explosives Ordnance Disposal Tech. Center Attn: Code D (Dr. L. Dickinson) Indian Head, MD 20304	1
Naval Sea Systems Command Attn: SEA-06G42 (Dr. R. Bowen) Washington, DC 20362	1
Naval Sea Systems Command Attn: SEA-62D31 (Mr. R. Cassel) Washington, DC 20362	1
Naval Weapons Center Attn: Code 38 (Dr. R.L. Derr) China Lake, CA 93555	1
Naval Weapons Center Attn: Code 3891 (Dr. M. Chan) China Lake, CA 93555	1
Naval Weapons Center Attn: Code 38503 (Dr. A. Neilson) China Lake, CA 93555	1

	Copies
Hercules Aerospace Co. Attn: Dr. E.H. Debutts P.O. Box 27408 Salt Lake City, UT 84127	1
Thiokol Corporation Attn: Mr. E.S. Sutton Elkton Division P.O. Box 241 Elkton, MD 21921	1
Morton Thiokol, Inc. Attn: Dr. G. Thompson Wasatch Division MS 240, P.O. Box 524 Brigham City, UT 84303	1
Morton Thiokol, Inc. Attn: Dr. T.F. Davidson Aerospace Group 110 North Wacker Drive Chicago, IL 60606	1
U.S. Army Research Office Chemical & Biological Sciences Division P.O. Box 12211 Research Triangle Park, NC 27709	1
Army Armament Research and Development Command Attn: DRSMC-LCE (Dr. J. Lannon) Dover, NJ 07801	1
Institute of Polymer Science Attn: Prof. A.N. Gent University of Akron Akron, OH 44325	1
University of California Attn: Prof. M.D. Nicol Dept. of Chemistry and Biochemistry 405 Hilgard Avenue Los Angeles, CA 90024	1

DISTRIBUTION (Cont.)

	Copies
Strategic Systems Project Office Department of the Navy Attn: Code SP-2731 (Mr. E.L. Throckmorton) Room 1048 Washington, DC 20376	1
Hercules Aerospace Div. Attn: Dr. K.O. Hartman Hercules Incorporated P.O. Box 210 Cumberland, MD 21502	1
Atlantic Research Corp. Attn: Dr. M.K. King 5390 Cherokee Avenue Alexandria, VA 22312	1
Aeroject Strategic Propulsion Co. Attn: Dr. R. Olsen Bldg. 05025 - Dept. 5400 MS 167 P.O. Box 15699C Sacramento, CA 95813	1
U.S. Army Research Office Attn: Dr. D. Mann Engineering Division Box 12211 Research Triangle Park, NC 27709-2211	1
JHU Applied Physics Lab Attn: CPIA Johns Hopkins Road Laurel, MD 20707	1
P. A. Miller 736 Leavenworth St.,#6 San Francisco, CA 94109	1
Naval Research Laboratory Attn: Code 6120 (Dr. W. Moniz) Washington, DC 20375	1
Georgia Institute of Technology Attn: Professor E. Price School of Aerospace Engr. Atlanta, GA 30332	1
Aerojet Strategic Propulsion Company Attn: R.B. Steel P.O. Box 15699C Sacramento, CA 95813	1
United Technologies Chemical Systems Attn: Dr. R.S. Valentini P.O. Box 50015 San Jose, CA 95150-0015	1
Naval Postgraduate School Attn: Code 012 (Dr. J. Wall) Director, Research Admin. Monterey, CA 93943	1
Morton Thiokol, Inc. Attn: L.C. Estabrook,P.E. P.O. Box 30058 Shreveport, LA 71130	1
Morton Thiokol, Inc. Attn: Dr. J.R. West P.O. Box 30058 Shreveport, LA 71130	1
Morton Thiokol, Inc. Attn: Dr. D.D. Dillehay Longhorn Division Marshall, TX 75760	1
Atlantic Research Corp. Attn: G.T. Bowman 7511 Wellington Road Gainesville, VA 22065	1
Atlantic Research Corp. Attn: R.E. Shenton 7511 Wellington Road Gainesville, VA 22065	1

DISTRIBUTION (Cont.)

	Copies
Ballistic Missile Defense Advanced Technology Center Attn: Dr. D.C. Sayles P.O. Box 1500 Huntsville, AL 35807	1
Naval Air Systems Command Attn: NAVAIR-320G Jefferson Plaza 1 Rm. 472 Washington, DC 20361	1
Atlantic Research Corp. Attn: B. Wheatley 7511 Wellington Road Gainesville, VA 22065	1
Massachusetts Institute of Technology Attn: Prof. J. Deutch Department of Chemistry Cambridge, MA 02139	1
Aerojet Strategic Propulsion Co. Attn: Dr. R. Peters Bldg. 05025 - Dept. 5400 MS 167 P.O. Box 15699C Sacramento, CA 95813	1
Morton Thiokol, Inc. Attn: D.A. Flanigan Director, Adv. Technologv Aerospace Group 110 North Wacker Drive Chicago, IL 60606	1
Naval Ordnance Station Attn: Code 5253 Indian Head, MD 20640	1
Aerojet Tactical Systems Attn: G.A. Zimmerman P.O. Box 13400 Sacramento, CA 95813	1

	Copies
Atlantic Research Corp. Attn: M. Barnes 7511 Wellington Road Gainesville, VA 22065	1
University of Maryland Attn: Dr. X.J. Zhang Dept. of Mechanical Engr. College Park, MD 20742	1
Los Alamos National Lab. Attn: B. Swanson INC-4, MS C-346 Los Alamos, NM 87545	1
Naval Weapons Center Attn: Code 3205 (Dr. J.T. Bryant) China Lake, CA 93555	1
Naval Weapons Support Ctr. Attn: Code 5063 (Dr. H. Webster,III) Manager, Chemical Sciences Branch Crane, IN 47522	1
Hercules, Inc. Attn: G. Butcher MS X2H P.O. Box 98 Magna, UT 84044	1
Atlantic Research Corp. Attn: W. Waesche 7511 Wellington Road Gainesville, VA 22065	1
Naval Air Systems Command Attn: AIR-320R Washington, DC 20361	1
The Johns Hopkins Univ. Attn: Dr. J.J. Kaufman Department of Chemistry Baltimore, MD 21218	1

DISTRIBUTION (Cont.)

	Copies
Air Force Office of Scientific Research Attn: Dr. A.J. Matuszko Directorate of Chemical and Atmospheric Sciences Bolling Air Force Base Washington, DC 20332	1
USA Ballistic Research Laboratory SLCBR-IB-P Attn: J.J. Rocchio Aberdeen Proving Ground, MD 21005-5066	1
Morton Thiokol, Inc. Attn: Dr. R.B. Kruse Huntsville Division Huntsville, AL 35807-7501	1
Naval Ordnance Station Attn: Code 5253K (J.A. Birkett) Indian Head, MD 20640	1
Naval Weapons Center Attn: Code 3891 (H. Richter) China Lake, CA 93555	1
SRI International Attn: J.T. Rosenberg 333 Ravenswood Avenue Menlo Park, CA 94025	1
SRI International Attn: D. Curran 333 Ravenswood Avenue Menlo Park, CA 94025	1
Lockheed Missiles & Space Company Attn: Dr. R. Martinson Research and Development 3251 Hanover Street Palo Alto, CA 94304	1
Rutgers University Attn: K.D. Pae High Pressure Materials Research Laboratory P.O. Box 909 Piscataway, NJ 08854	1
Los Alamos National Lab. Attn: Dr. J.K. Dienes T-3, B216 P.O. Box 1663 Los Alamos, NM 87544	1
SRI International Attn: Dr. D.A. Shockey 333 Ravenswood Avenue Menlo Park, CA 94025	1
Texas A&M University Attn: Prof. R.A. Schapery Dept. of Civil Engineering College Station, TX 77843	1
Washington State Univ. Attn: Prof. G.D. Duvall Department of Physics Pullman, WA 99163	1
Washington State Univ. Attn: Prof.J.T. Dickinson Department of Physics Pullman, WA 99163	1
University of Maryland Attn: Prof.R.W. Armstrong Dept. of Mechanical Engr. College Park, MD 20742	25
Office of Naval Technology Attn: ONT-21 (Dr. E. Zimet) Arlington, VA 22217	1
Brimrose Corp. of America Attn: Dr. R.G. Rosemeier 7720 Belair Road Baltimore, MD 21236	1

DISTRIBUTION (Cont.)

	Copies
Washington State Univ. Attn: Prof. M.H. Miles Department of Physics Pullman, WA 99163	1
Lockheed Palo Alto Research Laboratory Attn: G.A. Lo B204 Palo Alto, CA 94304	1
Morton Thiokol, Inc. Attn: G.E. Manser Wasatch Division P.O. Box 524 Brigham City, UT 84302	1
Pennsylvania State Univ. Attn: Prof. K. Kuo Dept. of Mechanical Engineering University Park, PA 16802	1
University of Delaware Attn: Prof. T.B. Brill Department of Chemistry Newark, DE 19716	1
Strategic Systems Project Office Department of the Navy Attn: Code SP-27311 (Mr. J. Culver) Room 1048 Washington, DC 20376	1
Naval Research Laboratory Attn: Code 6360 (Dr. C.Cm. Wu) Washington, DC 20375	1
Los Alamos National Lab. Attn: Dr. H. Cady MS 920 Los Alamos, CA 87545	1

	Copies
National Bureau of Standards Attn: Dr. M. Kuriyama Bldg. 223, Room B266 Washington, DC 20234	1
Naval Weapons Center Attn: Code 3853 (Dr. R.Y. Yee) China Lake, CA 93555	1
Naval Weapons Center Attn: Code 389 (Mr. T. Boggs) China Lake, CA 93555	1
Space Sciences, Inc. Attn: Dr. M. Farber 135 Maple Avenue Monrovia, CA 91016	1
New Mexico Institute of Mining & Technology Attn: Dr. K.R. Brower Department of Chemistry Socorro, NM 87801	1
Sandia National Laboratory Attn: Dr. R. Behrens Combustion Research Lab. Livermore, CA 94550	1
Sandia National Laboratory Attn: Dr. C.F. Melius Division 8357 Livermore, CA 94550	1
Loyola College Attn: Mr. T.E. Scheye Provost's Office 4501 N. Charles Street Baltimore, MD 21210	1
Loyola College Attn: Dean D.F. Roswell College of Arts & Sciences 4501 N. Charles Street Baltimore, MD 21210	1

DISTRIBUTION (Cont.)

	Copies
Washington State Univ. Attn: Prof. Y. Gupta Department of Physics Pullman, WA 99163	1
Naval Research Lab. Attn: Director Code 2627 Washington, DC 20375	1
Univ. of New Orleans Attn: Prof. P. Politzer Department of Chemistry New Orleans, LA 70148	1
AFATL/MNE Attn: Dr. N. Klausutis Eglin AFB, FL 32542	1
Office of Naval Research Attn: Administration Contracting Officer, (Mr. M.T. McCracken) 8th Floor 818 Connecticut Ave., NW Washington, DC 20036	1
Loyola College Attn: Prof.P.J.Coyne,Jr. Dept. of Engineering Sci. 4501 N. Charles Street Baltimore, MD 21210	10
Loyola College Attn: Prof. W.L. Elban Dept. of Engineering Sci. 4501 N. Charles Street Baltimore, MD 21210	25
University of Maryland Attn: Prof. H.L. Ammon Department of Chemistry College Park, MD 20742	1
NSACSS Attn: G74(TA) Ft. George G. Meade, MD 20755	1

Internal Distribution:	Copies
R	1
R10	1
R101	1
R11	1
R11 (Chaykovksy)	1
R11 (Doherty)	1
R11 (Gotzmer)	1
R11 (Leahy)	1
R11 (Ringbloom)	1
R12	1
R10B	1
R10C	1
R10D	1
R10E	1
R10F	1
R13	1
R13 (Clairmont)	1
R13 (Coffey)	1
R13 (DeVost)	1
R13 (Forbes)	1
R13 (Glancy)	10
R13 (Jacobs)	1
R13 (Jones)	1
R13 (Miller)	1
R13 (Price)	1
R13 (Sandusky)	10
R14	1
R15	1
R16	1
R16 (Consaga)	1
R16 (Carlson)	10
R341 (Beard)	1
R341 (Sharma)	1
E35	1
E231	2
E232	15